Computer Communications 201 (2023) 1–19

Contents lists available at ScienceDirect

Computer Communications

journal homepage: www.elsevier.com/locate/comcom

Joint energy and throughput optimization for MEC-enabled multi-UAV IoRT networks

Sriharsha Chigullapally [a,*], C. Siva Ram Murthy [b]

[a] Department of Computer Science and Engineering, Indian Institute of Technology Madras, Chennai, India
[b] Department of Computer Science and Engineering, Indian Institute of Technology Hyderabad, Hyderabad, India

ARTICLE INFO

Keywords:
IoRT
SAGIN
UAV
MEC
Connection scheduling
Power scheduling
Trajectory design
Bit transmission scheduling
Bandwidth allocation

ABSTRACT

In this paper, we study an Unmanned Aerial Vehicle (UAV) enabled Mobile Edge Computing (MEC) service provisioning to the Internet of Remote Things (IoRT) devices spread randomly on the ground in a remote area. The data generated by the IoRT devices is collected by the UAVs, which immediately relay the data collected to an MEC device installed on the ground at a nearby location. The MEC device receives the data from the UAVs, and sends the results back to the UAVs, which in turn relay them to IoRT devices. We aim to minimize the energy consumption by the IoRT devices and the UAVs, while maximizing the system throughput subject to bandwidth, power, information-causality, and UAVs' trajectory constraints. We formulate the problem as a Mixed Integer Non Linear Programming problem, which is a complex and non-convex optimization problem. To make the problem tractable, we use variable relaxation. We further develop an iterative algorithm based on Block Coordinate Descent method, to jointly optimize the connection scheduling, power control, bit transmission scheduling, bandwidth allocation, and trajectories of the UAVs. Numerical results demonstrate the convergence of the algorithm and superiority of the proposed model with respect to conventional methods. Our proposed system model of placing MEC at ground shows 9% improvement in energy consumption when compared to carrying out computations at MEC carried by UAV and a 99% improvement when compared to placing MEC at the satellite. The proposed system model shows a 0.2% lower system throughput on average, compared to placing MEC at UAV, which is tolerable considering gains in terms of energy consumption.

1. Introduction

With the deployment of 5G being rolled out across the world, the research community is already looking towards the next generation of wireless communication. The 6G networks envision, among other things, ubiquitous global network coverage i.e., coverage of even remote areas in the world such as deserts, high seas and isolated islands [1]. Coverage in remote areas of the planet has high value in various applications such as tracking of global cargo movement, military reconnaissance and surveillance, weather monitoring and forewarning of calamities, and regular monitoring of climate in remote terrain for environmental studies. In these use cases, the Internet of Remote Things (IoRT) devices can be deployed in a remote area to collect data about the surrounding environment. The data, for instance, can be multimedia images in case of military surveillance, which needs processing to assess any possible threats. The data from the IoRT devices needs to be analyzed by a computing device, which can determine the action that needs to be taken, for instance, instructions to IoRT devices based on the inputs. To enable provisioning of computing services to remote devices, various architectures and solutions have been proposed, one promising architecture among which is Space–Air–Ground Integrated Network (SAGIN), which makes use of Low Earth Orbit (LEO) satellites and High Altitude Platforms (HAP). The SAGIN enables the connectivity of the IoRT devices which are deployed in remote areas and the provisioning of computing facilities to the IoRT devices through Mobile Edge Computing (MEC). It is economically infeasible to connect the remote areas, where the network demand is usually very low, to mainland using optical fiber network. Hence, to handle the processing of data collected from IoRT devices in remote areas, various SAGIN based system models have been proposed in the literature to provide MEC to the IoRT devices using Unmanned Aerial Vehicles (UAVs) and LEO satellites.

When using UAVs to enable the processing of data collected from IoRT devices, there are two main locations where the computing device i.e, MEC can be placed. The first location for MEC placement is the LEO satellite, wherein the UAVs can be used to relay the data received from the IoRT devices the MEC device place in the satellite. To illustrate, the authors in [2,3] used UAVs as relays for uploading the data from ground devices to LEO satellites and optimized energy efficiency and

* Corresponding author.
E-mail address: cs17d012@cse.iitm.ac.in (S. Chigullapally).

https://doi.org/10.1016/j.comcom.2023.01.012
Received 4 September 2022; Received in revised form 9 January 2023; Accepted 15 January 2023
Available online 18 January 2023

system throughput, respectively i.e, MEC is placed at the satellite. Alternately, the MEC can be placed at the UAVs, i.e., the UAVs carry MEC devices and provide computing services to the IoRT devices. In [4], UAVs are used as edge computing devices for IoRT devices, with basic computing capabilities and satellites are used as cloud. Even in [5,6], UAVs carry MEC devices and provide computation services. In [7,8], UAV performs part of the computations while relays the rest to an access point and an edge cloud respectively. However, both the placements of MEC - at the satellite and at the UAV are energy inefficient. Since the UAVs are power constrained devices, sending all the data to satellite is costly and may not be actually needed all the time. Similarly, carrying out computation on energy-critical UAV devices could drain out the UAVs and also result in frequent trips to charging stations. In our work, we propose an alternate placement for MEC device, i.e., on the ground nearby, to which the UAVs relay the data collected from the IoRT devices. For the purpose of this work, we consider only delay tolerant data.

It is important in various applications such as tracking of global cargo movement and military surveillance to send the control commands back to the IoRT devices. However, most of the existing works in the literature focus only the data collection from IoRT devices and ignore the delivery of results back to the IoRT devices. In [9], the UAVs are used to collect data from IoRT devices. Depending on the delay sensitivity of the data, the UAVs either store-and-carry the data or relay to the LEO satellite. An aerial mesh network of UAVs is proposed by authors of [10] to collect the data from ground IoT devices in a remote geographic area and relay the collected data to cloud for further processing. The architecture proposed in [11] uses UAVs to perform wireless power transfer and also collect data from IoT devices deployed in remote and disaster areas. In contrast to the data collection by UAV, our work also considers the sending of computed results back to IoRT devices. In addition, we consider the dual objective of minimizing the energy consumption and maximizing the system throughput.

The contributions of this paper are listed below:

- We propose an alternate and energy efficient location for MEC placement in the Space–Air–Ground integrated network for provisioning MEC services to the IoRT devices spread over a remote area.
- We formulate the problem which captures the end-to-end data movement, i.e, from IoRT devices to MEC device via UAV and back. The formulated problem tries to achieve the dual objective of minimizing the energy consumption of UAVs and IoRT devices as well as maximizing the system throughput.
- To achieve the dual objective of minimizing energy consumption and maximizing the average system throughput, we perform joint optimization of connection scheduling, power control, bit transmission scheduling, bandwidth allocation and trajectories of the UAVs.
- We propose an iterative solution for the formulated problem based on Block Coordinate Descent (BCD) method. Using detailed numerical simulations, we demonstrate the effectiveness of the proposed solution.

The remainder of the paper is organized as follows. Section 2 presents the system model and problem formulation. Section 3 describes the solution proposed, while Section 4 discusses the numerical simulation details and observations made. Finally, Section 5 concludes the paper.

2. Related work

UAVs have been variously used in enhancing the communication, both in remote and non-remote areas. The existing literature on UAVs focuses on optimizing various aspects of UAV communication such as the energy consumption of the UAVs, the system throughput, the overall system delay, interference mitigation, and the overall system computation rate. Various relevant optimization problems are considered such as optimization of channel allocation, computing resource allocation, offloading ratio, hovering duration, trajectory, placement of the UAVs, connection scheduling, bit allocation, bandwidth allocation, and power control. The UAVs are also studied for their integration in SAGIN and enabling edge computing.

In this section, we give a survey of the current state of the art and highlight the lacunae observed in the state of the art which we try to address. To start with, the placement of the MEC location in the existing literature is not energy-efficient. To provide MEC services to remote devices using SAGIN architecture, the MEC device has been proposed to be placed either at UAV i.e, aerial layer or at satellite i.e, space layer or in both locations. Placing MEC on the ground is more energy efficient compared to the other two locations, as we explain further in this section. In the few works which locate MEC on the ground, the system models used have the drawback of either performing computations partly at the UAV which is also energy inefficient or requiring that the users offload the data themselves to the MEC which is not feasible for remote locations. It is also observed that the works which located MEC on the ground did not consider the minimization of energy consumption and maximization of system throughput jointly, both important objectives for the use case of provisioning MEC services to IoRT devices. In addition, we consider multi-UAV scenario and two-way movement of data in our problem formulation i.e., from the IoRT devices to the MEC and back, which has been missing in the current literature.

In [12], the MEC is placed in both UAV and satellites. In [4], UAVs are used as edge computing devices for IoRT devices, with basic computing capabilities and satellites are used as cloud. The users can relay their data to either UAV or satellite. In [2,3], UAVs are used as relays for uploading the data from ground devices to LEO satellites i.e, MEC is placed at the satellite. However, placing MEC at satellites is not energy-efficient, as relaying to satellites incurs huge energy consumption.

Alternately, the MEC can be placed at the UAVs, i.e., the UAVs carry MEC devices and provide computing services to the IoRT devices. Even in [5,6], UAVs carry MEC devices and provide computation services. UAVs carry out the computation in the system models used in [13–21]. In [13], the authors minimized the average delay of the user devices, which are mobile, by jointly offloading the movements of user devices and the offloading variables. The problem formulated in [14] maximizes the computation bits of the mobile terminals while ensuring fairness among them. The authors in [15–17] attempted to minimize the energy consumption, while [18,19] minimize the task completion and average time delay of the user respectively. In [20,21], the number of served IoT devices and rate of served requests are maximized respectively. When UAVs carry out the computation as in [13–21], there is a faster depletion of energy at the UAV due to three reasons. First, the computation requires energy, which can be high in use cases such as military surveillance where computation-intensive tasks such as image processing may have to be done. Second, the UAV has to carry MEC device which increases the weight of the UAV and hence the flying energy. Third, the faster depletion of energy leads to frequent trips to the charging station, leading to further energy inefficiency.

In [22–24], MEC is placed at UAVs along with ground servers. However, the users have to offload their tasks to either UAVs or the ground servers. In the use cases where the users are not in the vicinity of the ground servers, direct offloading is not feasible to implement. Alternately, in [7,8], UAV performs part of the computations while relaying the rest to an access point and an edge cloud respectively. Similar system model is also used in [25–28], wherein the UAV performs part of computation and offloads the rest of the computation to an edge cloud or an MEC device which is located at a base station or at an access point. As explained above, in all the cases where computation is carried out at UAV, the energy available at the UAV depletes faster, resulting in overall energy inefficiency.

In [29], multiple UAVs are used to communicate with multiple terrestrial IoT devices. The authors of [29] formulated UAV deployment problem with multiple objectives of minimizing the energy consumption of the UAVs, maximizing the minimum system throughput of the UAV-device pairs and maximizing the total system throughput. However, the considered system model only considered the downlink communication and no computation of collected data was considered. Essentially, UAVs are used as the data delivery agents that transmit the data to IoT devices using Fly-Hover-Communicate protocol. In our work, we consider end-to-end data movement i.e., the data relaying from IoRT devices to MEC device using UAVs and the delivery of output data from MEC device to the IoRT devices. In most of the existing literature, the UAVs are used to do either data collection or data dissemination. Although the authors in [30,31] include the returning of results in their problem formulation, the computation is carried out at the UAVs, which is not energy efficient.

In this paper, we propose an alternate and energy efficient location for MEC placement in the SAGIN architecture — on the ground. We propose placing an MEC device on the ground nearby to provide centralized MEC services to the IoRT devices. The data from the IoRT devices is collected using UAVs and relayed to the MEC device installed nearby. Placing MEC at the ground is energy efficient compared to other two placements. Compared to placing the MEC at satellite, placing MEC on ground at a nearby location reduces the relaying distance and hence the energy consumption. Similarly, placing MEC on ground is efficient compared to placing it on UAV, as the UAVs need not expend energy to carry the MEC device or to perform the computations or to do frequent trips to charging stations that arise because of faster depletion of energy.

We consider a multi-UAV enabled MEC service provisioning to IoRT devices that are spread over remote location. We formulate the problem to achieve the dual objective of minimizing the energy consumption while maximizing the system throughput. We also account for the end-to-end data movement in our problem formulation. We propose a solution that optimizes the connection scheduling, the power levels of IoRT devices and the UAVs, bit transmission scheduling, bandwidth allocation and trajectories of the UAVs, while jointly minimizing the energy consumption and maximizing the throughput. We then perform detailed numerical simulations to evaluate the performance of our solution.

We summarize the comparison of the state of the art and our work in the Table 1. To our best knowledge, joint optimization of energy consumption and system throughput in a multi-UAV enabled MEC for remote IoRT devices has not been considered before.

3. System model and problem formulation

3.1. System model

The data from IoRT devices in the remote area is collected with the help of UAVs. The IoRT devices offload the data to the UAVs, which immediately relay the data received to the MEC device installed on the ground. The computations are performed at the MEC device and the results are returned to the IoRT devices using UAV. The system model described is illustrated in Fig. 1.

We consider M UAVs with Amplify and Forward (AF) relays to be flying in the air, which collect data from the IoRT devices and forward it to the MEC device. We choose AF relays over decode and forwarding because the channel conditions are better in remote locations compared to urban scenarios. Moreover, the UAVs do not do any computation or any decision making regarding the processing of data. The UAVs just relay the data that is received from the IoRT devices to the MEC device and hence no decoding is necessary. The UAVs do not have any direct communication between them. We consider all the UAVs to be in line of sight of the MEC device and hence all the UAVs directly transmit to the MEC device. The connection scheduling and bit transmission scheduling for a given time slot is calculated and shared with the UAVs and IoRT devices.

Let us denote the set of IoRT devices by $\mathcal{K} = \{1, 2, 3, \dots, K\}$ and the set of UAVs by $\mathcal{M} = \{1, 2, 3, \dots, M\}$, where K and M represent the number of IoRT devices and the number of UAVs, respectively. We consider that identical frequency band is shared by the UAVs and the IoRT devices within a time duration $\mathscr{T}$ [3]. The 2 Dimensional (2D) coordinates of the IoRT devices on the ground are represented by $\mathbf{w_k} = [x_k, y_k]^T \in \mathcal{R}^{2\times1}, k \in \mathcal{K}$. We assume that all the UAVs fly at the fixed height H [4], the minimum height that is required for the safety considerations. Let the antenna of the MEC device is at the height H_m and at the horizontal location $\mathbf{w}_M = [x_M, y_M]^T \in \mathcal{R}^{2\times1}$.

3.1.1. Trajectory model

The entire time duration $\mathscr{T}$ is divided in to T time slots of equal length, $\Delta = \frac{\mathscr{T}}{T}$. The time slots are $t \in \mathcal{T} = \{1, 2, \dots, T\}$. We also define the set $\mathcal{T}_1 = \{1, \dots, T-1\}$. The 2D position of mth UAV in tth time slot is represented by $\mathbf{u}_m[t] = [x_m[t], y_m[t]]^T \in \mathcal{R}^{2\times1}, m \in \mathcal{M}, t \in \mathcal{T}$. Therefore, we can express the UAV flight trajectory as $\{\mathbf{u}_m[t]\}|_{t=1}^{T}$. The constraints that should be met by the UAV trajectory are given by:

$$\mathbf{u}_m[1] = \mathbf{u}_m[T], \forall m \tag{1}$$

$$\|\mathbf{u}_m[t+1] - \mathbf{u}_m[t]\|^2 \le (V_{max}\Delta)^2, \forall m, t \in \mathcal{T}_1 \tag{2}$$

$$\|\mathbf{u}_m[t] - \mathbf{u}_j[t]\|^2 \ge d_{\min}^2, \forall m, j \ne m, t \in \mathcal{T} \tag{3}$$

The Eq. (1) implies that the UAV should come back to its initial position at the end of each time duration $\mathscr{T}$, so that the IoRT devices can be served periodically in the next time duration [32]. It also enables the UAVs to get charged at the starting locations and fly again [6]. The Eq. (2) is constraint on the distance covered by the UAV in each time slot when it flies at the maximum speed (V_{max}), where in $\|.\|$ represents the Euclidean norm. Eq. (3) is the safety constraint of the UAVs. The UAVs should fly with a minimum distance between each of them of at-least d_{min}, to avoid collisions.

3.1.2. Throughput model

Let $P_{k,m}^{D\to U}[t]$ represent the transmission power of the kth IoRT device to the mth UAV in the tth time slot. The corresponding channel gain is represented by $h_{k,m}^{D\to U}[t]$ and distance is $d_{k,m}^{D\to U}[t]$. The transmission power between the mth UAV and the MEC device in the tth time slot is represented by $P_m^{U\to M}[t]$. Corresponding channel gain is $h_m^{U\to M}[t]$ and distance is $d_m^{U\to M}[t]$. The symbol h_0 denotes the channel gain at a reference distance of 1 m.

We avoid interference among the IoRT devices and the UAVs by adopting a periodic time division multiple access (TDMA) protocol. We choose TDMA over non orthogonal multiple access as the latter is highly energy-consuming. We assume that the wireless channels between the UAV and the MEC device as well as the IoRT devices are dominated by LoS links, as observed in the field experiments done by Qualcomm [33]. Therefore, the transmission channel gain and signal-to-noise ratio (SNR) of the kth IoRT device to the mth UAV in the tth time slot are given by

$$h_{k,m}^{D\to U}[t] = h_0(d_{k,m}^{D\to U}[t])^{-2} = \frac{h_0}{H^2 + \|\mathbf{u}_m[t] - \mathbf{w}_k\|^2} \tag{4}$$

$$\gamma_{k,m}^{D\to U}[t] = \frac{P_{k,m}^{D\to U}[t] h_{k,m}^{D\to U}[t]}{\sigma^2}, \tag{5}$$

where σ^2 denotes the noise power at the UAV[1]. We assume that there is channel reciprocity in the considered system model and thus the uplink and downlink channels between the IoRT devices and UAVs are identical [7].

[1] For the ease of analysis, we consider the noise power at any node in the system to be the same as σ^2

Table 1
Comparison with the state of the art.

Work	Objective		System model				
	Energy	Throughput	Multi-UAV	2-way data flow	Remote scenario	MEC location	Description
[2]	✓	✓	✓	✗	✓	LEO satellite	UAVs relay the data from ground devices to the LEO satellite.
[3]	✗	✓	✓	✗	✓	LEO satellite	Energy consumed to relay data to satellite is very high.
[4]	✓	✗	✓	✗	✓	UAV and satellite	Users should relay data to either UAV-MEC or satellite-cloud (energy-intensive).
[5,6]	✓	✗	✗	✗	✗	UAV	UAV has MEC device on board and serves the users/IoT devices on the ground.
[7]	✓	✗	✗	✗	✓	UAV and access point	UAV performs part of the computations and offloads the rest to access point.
[8]	✓	✗	✗	✗	✗	UAV and edge clouds	UAV performs part of the computations and offloads the rest to edge cloud. Objective also includes minimizing total service delay.
[15]	✓	✗	✗	✗	✗	UAV	Specific use case of federated learning.
[16]	✓	✗	✗	✗	✗	UAV	Partial offloading is done to UAV.
[17]	✓	✗	✗	✗	✓	UAV	Energy consumption of only UAV is minimized, not of the devices.
[19]	✗	✗	✗	✗	✗	UAV, ground base station	The task is offloaded either to the ground base station or to the UAV - objective is to minimize the time delay.
[20]	✗	✗	✓	✗	✗	UAV	The number of devices served is maximized.
[21]	✗	✗	✓	✗	✗	UAV	Objective is to maximize the rate of served requests.
[30]	✓	✗	✗	✓	✗	UAV	Tasks are partially offloaded to UAV. When UAV provides MEC services, energy efficiency is low as the UAV should expend energy to carry MEC device, to perform computations and also to do extra trips to the charging station due to faster draining of battery.
[22]	✓	✗	✓	✗	✗	UAV and base station	Joint optimization of latency and energy consumption. The task is offloaded by the user to either UAV or base station directly. Hence, this system model is not suitable for low power devices such as IoRT devices as the energy required to transmit from device to base station could be high.
[23]	✓	✗	✗	✓	✗	UAV and access points	The user should offload to the UAV or access point. Hence, it is not suitable for low power devices.

(*continued on next page*)

Table 1 (*continued*).

Work	Objective		System model				
	Energy	Throughput	Multi-UAV	2-way data flow	Remote scenario	MEC location	Description
[24]	✓	✗	✗	✗	✗	UAV and base station	Joint optimization of latency and energy consumption. Users should offload to the UAV or base station directly. The system model is not suitable for low power devices.
[25]	✓	✗	✗	✗	✗	UAV and access point	UAV performs partial or full offloading to the MEC at access point.
[26]	✓	✗	✓	✗	✗	UAV and base station	Energy consumption of mobile user devices is minimized, but not of the UAV.
[27]	✓	✗	✗	✗	✗	UAV and edge clouds	UAV serves as both relay device and also MEC device. Objective includes the minimization of service delay also.
Our work	✓	✓	✓	✓	✓	Ground	UAVs relay the data collected from the IoRT devices to the MEC device installed on the ground. We also consider end-to-end data movement i.e., movement of data from IoRT devices to MEC device via UAV and movement of results back to the IoRT devices. We minimize the energy consumption by both IoRT devices and UAVs, while maximizing the system throughput. Our system model is suitable for remote areas.

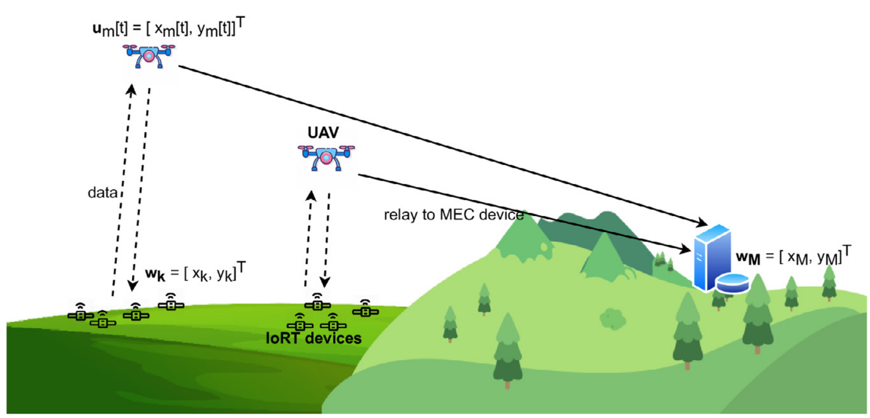

Fig. 1. System model.

Similarly, the transmission channel gain and SNR of the mth UAV to the MEC device in the tth time slot is given by

$$h_m^{U\to M}[t] = h_0(d_m^{U\to M}[t])^{-2} = \frac{h_0}{(H-H_m)^2 + \|\mathbf{u}_m[t] - \mathbf{w}_M\|^2} \tag{6}$$

$$\gamma_m^{U\to M}[t] = \frac{P_m^{U\to M}[t]h_m^{U\to M}[t]}{\sigma^2}, \tag{7}$$

Following the Shannon formula and AF protocol [34], the transmission rate when the data from the kth IoRT device is relayed to the MEC device through the mth UAV in the tth time slot is given by,

$$R_{k,m}[t] = Blog_2(1 + \frac{\gamma_{k,m}^{D\to U}[t]\gamma_m^{U\to M}[t]}{1+\gamma_{k,m}^{D\to U}[t]+\gamma_m^{U\to M}[t]}) \tag{8}$$

We use a binary variable $c_{k,m}[t]$ to indicate the connection between kth IoRT device and mth UAV in tth time slot, which is equal to 1 if connected so and 0 otherwise. We assume that not more than one IoRT device is served by each UAV and each IoRT device is served by not more than one UAV [3] in each time slot. Hence, we have

$$\sum_{k=1}^{K} c_{k,m}[t] \le 1, \forall m,t \tag{9}$$

$$\sum_{m=1}^{M} c_{k,m}[t] \leq 1, \forall k, t \tag{10}$$

and

$$c_{k,m}[t] \in \{0,1\}, \forall k, m, t \tag{11}$$

The coverage constraint of the UAV can be expressed as

$$c_{k,m}[t]\|\mathbf{u}_m[t] - \mathbf{w}_k\| \leq H \cot\theta, \forall k, m, t, \tag{12}$$

where θ is the UAV angle and $H cot\theta$ represents the coverage radius.

The average throughput for the time duration $\mathcal{T}$ is given by

$$R_{k,m} = \frac{1}{T}\sum_{t=1}^{T} c_{k,m}[t]R_{k,m}[t] \tag{13}$$

3.1.3. Energy consumption model

Energy is consumed for the transmission of the collected data and results, and also for flying the UAV. We ignore the energy consumed for computation as the computation is done only at MEC device which is not energy critical [7] as it is considered to be connected to a stable power source.

Energy consumed for transmission. To use the TDMA protocol, we further divide the time slot Δ into K small time slots each of duration $\delta = \Delta/K$. The kth IoRT device offloads its data in the kth small time slot. Let the data generated at the kth IoRT device measured in bits be L_k, which is transmitted to the UAV it is connected to. Let $l^{D\to U}_{k,m}[t]$ denote the number of bits of data generated at the kth IoRT device in time slot t and transmitted to mth UAV to which it is connected to in its allocated duration. The UAV immediately relays all the bits to the MEC device for computation.

1. Offloading from IoRT device to UAV: Based on standard information-theoretic arguments [35], the energy consumed for offloading $l^{D\to U}_{k,m}[t]$ number of bits from kth IoRT device to mth UAV in the tth time slot is given by

$$E^{D\to U}_{k,m}[t] = \frac{\delta\sigma^2}{h^{D\to U}_{k,m}[t]}\left(2^{\frac{l^{D\to U}_{k,m}[t]}{\delta B^{D\to U}_{k,m}[t]}} - 1\right), \tag{14}$$

where $B^{D\to U}_{k,m}[t]$ is the bandwidth allocated for offloading from kth IoRT device to mth UAV in tth time slot.

2. Offloading from UAV to MEC device: Energy consumed for offloading the $l^{U\to M}_{k,m}[t]$ number of bits received from kth IoRT device by mth UAV to the MEC device in the tth time slot is given by

$$E^{U\to M}_{k,m}[t] = \frac{\delta\sigma^2}{h^{U\to M}_{m}[t]}\left(2^{\frac{l^{U\to M}_{k,m}[t]}{\delta B^{U\to M}_{k,m}[t]}} - 1\right), \tag{15}$$

where $B^{U\to M}_{k,m}[t]$ is the bandwidth allocated for offloading ($l^{U\to M}_{k,m}[t]$ bits of) the data received from kth IoRT device by mth UAV to MEC device in tth time slot.

3. Downloading from MEC to UAV: As MEC device is not energy critical and the size of computing results is very small, we neglect energy consumed for downloading the results from MEC to UAV [7].

4. Downloading from UAV to IoRT device: Energy required to download $l^{U\to K}_{k,m}[t]$ number of bits from mth UAV to kth IoRT device in the tth time slot is given by

$$E^{U\to K}_{k,m}[t] = \frac{\delta\sigma^2}{h^{D\to U}_{k,m}[t]}\left(2^{\frac{l^{U\to K}_{k,m}[t]}{\delta B^{U\to K}_{k,m}[t]}} - 1\right), \tag{16}$$

where $B^{U\to K}_{k,m}[t]$ is the bandwidth allocated for downloading from mth UAV to kth IoRT device in tth time slot.

Energy required for flying the UAV. We assume that the length of the time slot Δ is sufficiently small such that the UAV can be considered to be flying with constant speed $v[t]$. For computing the energy consume for flying, we use adopt the simplified energy consumption model used in the existing literature [5,13,36]. The flying energy consumption for the mth UAV at time slot t, which depends on the velocity and weight of the UAV, is given by

$$E^{f}_{m}[t] = c\|v_m[t]\|^2 \tag{17}$$

$$v_m[t] = \frac{\mathbf{u}_m[t+1] - \mathbf{u}_m[t]}{\Delta}, \tag{18}$$

where $c = 0.5Q\Delta$, with Q representing the mass of a UAV.

The total energy consumption is given by

$$\begin{aligned} E =& w_1\left(\sum_{m=1}^{M}\sum_{k=1}^{K}\sum_{t=1}^{T} c_{k,m}[t]E^{D\to U}_{k,m}[t]\right)+ \\ & w_2\left(\sum_{m=1}^{M}\sum_{k=1}^{K}\sum_{t=1}^{T}(E^{U\to M}_{k,m}[t] + c_{k,m}[t]E^{U\to K}_{k,m}[t]) + \sum_{m=1}^{M}\sum_{t=1}^{T} E^{f}_{m}[t]\right), \end{aligned} \tag{19}$$

where $w_1, w_2 \in [0,1]$ are the weight factors of the energy consumption of the IoRT devices and the UAVs, respectively.

3.1.4. Bandwidth constraint

The UAV operates in a frequency-division-duplex (FDD) mode in each small time slot δ with separate bandwidths allocated for receiving data from the IoRT device, relaying it to the MEC device and sending the results back to the IoRT device, with a total bandwidth B available to it. The corresponding constraint is given by

$$B^{D\to U}_{k,m}[t] + B^{U\to M}_{k,m}[t] + B^{U\to K}_{k,m}[t] \leq B, k \in \mathcal{K}, m \in \mathcal{M},\ t \in \mathcal{T} \tag{20}$$

3.1.5. Information-causality constraints

It is to be noted that for $l^{U\to M}_{k,m}[t]$ input bits, $O_k l^{U\to M}_{k,m}[t]$ number of output bits are generated in the result after the computation. We assume that the computing time at the MEC device and the upload transmission time from the MEC device to the UAV are negligible [7]. Hence, the MEC device sends the computation results back to the UAV using a separate bandwidth within the same time slot using TDMA . The information-causality constraints for the transmission of the data between IoRT devices, UAV and MEC device are given by the Eqs. (21) and (22), where $\mathcal{T}_2 = \{2,\dots,T-1\}$ and $\mathcal{T}_3 = \{3,\dots,T\}$.

$$\sum_{i=2}^{t} l^{U\to M}_{k,m}[i] \leq \sum_{i=1}^{t-1} l^{D\to U}_{k,m}[i], \forall k, m, t \in \mathcal{T}_2, \tag{21}$$

$$\sum_{i=3}^{t} l^{U\to K}_{k,m}[i] \leq O_k \sum_{i=2}^{t-1} l^{U\to M}_{k,m}[i], \forall k, m, t \in \mathcal{T}_3, \tag{22}$$

The notations used in the system model are summarized in the Table 2 for the ease of reference.

3.2. Problem formulation

Let $\mathbf{C} = \{c_{k,m}[t], \forall k, m, t\}$, $\mathbf{U} = \{u_m[t], \forall m, t\}$, $\mathbf{P}^{D\to U} = \{P^{D\to U}_{k,m}[t], \forall k, m, t\}$ and $\mathbf{P}^{U\to M} = \{P^{U\to M}_{m}[t], \forall m, t\}$. Let $\mathbf{B} = \{\mathbf{B}_k[t], \forall k, t\}$, where $\mathbf{B}_k[t] = \{B^{D\to U}_{k,m}[t], B^{U\to M}_{k,m}[t], B^{U\to K}_{k,m}[t], \forall m\}$. We also define $\mathbf{L} = \{l_k[t], \forall k, t\}$, where $l_k[t] = \{l^{D\to U}_{k,m}[t], l^{U\to M}_{k,m}[t], l^{U\to K}_{k,m}[t], \forall m\}$. The 2D coordinates of the IoRT devices are assumed to be known. We adopt the trajectory initialization scheme from [32]. The goal is to maximize the throughput while minimizing the energy consumption by jointly optimizing the IoRT devices connection scheduling ($\mathbf{C}$), the UAV trajectory design ($\mathbf{U}$), the transmission power of IoRT devices ($\mathbf{P}^{D\to U}$), the transmission power of UAVs ($\mathbf{P}^{U\to M}$), the bandwidth allocation ($\mathbf{B}$) and the bit transmission scheduling ($\mathbf{L}$). The optimization problem is formulated as the problem (23).

$$\min_{\{\mathbf{C},\mathbf{U},\mathbf{P}^{D\to U},\mathbf{P}^{U\to M},\mathbf{B},\mathbf{L}\}} E - \zeta\sum_{m=1}^{M}\sum_{k=1}^{K} R_{k,m}, \tag{23a}$$

Table 2
Notation Summary.

Symbol	Description
K, M	Number of IoRT devices, Number of UAVs respectively
H_m, H	Heights of the MEC device and the UAVs, respectively.
$\mathbf{w_k}, \mathbf{w}_M, \mathbf{u}_m[t]$	Horizontal positions of the kth IoRT device located on the ground, the MEC device, and the mth UAV (in the nth time slot), respectively.
$\mathcal{T}, T, \Delta$	The length of entire time duration, the number of time slots, the length of each time slot, respectively
V_{max}, θ	The maximum speed of UAV, the UAV angle
d_{min}	The minimum safety distance between different UAVs.
$P_{k,m}^{D\to U}[t]$, $h_{k,m}^{D\to U}[t]$, $\gamma_{k,m}^{D\to U}[t]$	The transmission power, channel gain and SNR respectively from the kth IoRT device to the mth UAV in the nth time slot.
$P_m^{U\to M}[t]$, $h_m^{U\to M}[t]$, $\gamma_m^{U\to M}[t]$	The transmission power, channel gain and SNR respectively between the mth UAV and the MEC device in the nth time slot.
h_0, B	The channel gain at a reference distance of 1 m, system bandwidth respectively
$P_{max}^{D\to U}$, $P_{max}^{U\to M}$	The maximum transmission power of IoRT devices and UAVs in the nth time slot.
σ^2	Noise power spectral density of additive Gaussian white noise.
$c_{k,m}[t]$ $l_{k,m}^{D\to U}[t]$, $l_{k,m}^{U\to K}[t]$	Connection scheduling between the kth IoRT device and mth UAV in nth time slot. Number of data bits transmitted by the kth IoRT device to the mth UAV, and mth UAV to the kth IoRT device, respectively, in nth time slot.
$l_{k,m}^{U\to M}[t]$	Number of data bits received from the kth IoRT device that are transmitted by the mth UAV to the MEC device in nth time slot.
$B_{k,m}^{D\to U}[t]$, $B_{k,m}^{U\to M}[t]$, $B_{k,m}^{U\to K}[t]$	Bandwidth allocated for offloading from kth IoRT device to mth UAV, mth UAV to MEC device and mth UAV to kth IoRT device respectively, in the nth time slot.

$$s.t.\ \sum_{k=1}^{K} c_{k,m}[t] \le 1, \forall m, t \tag{23b}$$

$$\sum_{m=1}^{M} c_{k,m}[t] \le 1, \forall k, t \tag{23c}$$

$$c_{k,m}[t] \in \{0,1\}, \forall k, m, t, \tag{23d}$$

$$0 \le P_{k,m}^{D\to U}[t] \le P_{max}^{D\to U}, \forall k, m, t, \tag{23e}$$

$$0 \le P_m^{U\to M}[t] \le P_{max}^{U\to M}, \forall m, t, \tag{23f}$$

$$\mathbf{u}_m[1] = \mathbf{u}_m[T], \forall m, \tag{23g}$$

$$\|\mathbf{u}_m[t+1] - \mathbf{u}_m[t]\|^2 \le (V_{max}\Delta)^2, \forall m, t \in \mathcal{T}_1, \tag{23h}$$

$$c_{k,m}[t]\|\mathbf{u}_m[t] - \mathbf{w}_k\| \le H \cot\theta, \forall k, m, t, \tag{23i}$$

$$\|\mathbf{u}_m[t] - \mathbf{u}_j[t]\|^2 \ge d_{\min}^2, \forall m, t, j \ne m, \tag{23j}$$

$$\sum_{k=1}^{K} L_k(1+O_k) \le \sum_{m=1}^{M}\sum_{k=1}^{K}\sum_{t=1}^{T} c_{k,m}[t] R_{k,m}[t], \forall k, \tag{23k}$$

$$\sum_{i=2}^{t} l_{k,m}^{U\to M}[i] \le \sum_{i=1}^{t-1} l_{k,m}^{D\to U}[i], \forall k, m, t \in \mathcal{T}_2, \tag{23l}$$

$$\sum_{i=3}^{t} l_{k,m}^{U\to K}[i] \le O_k \sum_{i=2}^{t-1} l_{k,m}^{U\to M}[i], \forall k, m, t \in \mathcal{T}_3, \tag{23m}$$

$$\sum_{t=2}^{T-1} l_{k,m}^{U\to M}[t] = \sum_{t=1}^{T-2} l_{k,m}^{D\to U}[t], \forall k, m, \tag{23n}$$

$$\sum_{t=3}^{T} l_{k,m}^{U\to K}[t] = O_k \sum_{t=2}^{T-1} l_{k,m}^{U\to M}[t], \forall k, m, \tag{23o}$$

$$\sum_{t=1}^{T}\sum_{m=1}^{M} c_{k,m}[t](l_{k,m}^{D\to U}[t] + l_{k,m}^{U\to K}[t]) = L_k(1+O_k), \forall k, \tag{23p}$$

$$B_{k,m}^{D\to U}[t] + B_{k,m}^{U\to M}[t] + B_{k,m}^{U\to K}[t] \le B, \forall k, m, t \tag{23q}$$

$$l_{k,m}^{D\to U}[T-1] = l_{k,m}^{D\to U}[T] = 0, l_{k,m}^{D\to U}[t] \ge 0, \forall k, m, t \in \mathcal{T}_1, \tag{23r}$$

$$l_{k,m}^{U\to M}[1] = l_{k,m}^{U\to M}[T] = 0, l_{k,m}^{U\to M}[t] \ge 0, \forall k, m, t \in \mathcal{T}_2, \tag{23s}$$

$$l_{k,m}^{U\to K}[1] = l_{k,m}^{U\to K}[2] = 0, l_{k,m}^{U\to K}[t] \ge 0, \forall k, m, t \in \mathcal{T}_3, \tag{23t}$$

$$B_{k,m}^{D\to U}[T-1] = B_{k,m}^{D\to U}[T] = 0, B_{k,m}^{D\to U}[t] \ge 0, \forall k, m, t \in \mathcal{T}_1, \tag{23u}$$

$$B_{k,m}^{U\to M}[1] = B_{k,m}^{U\to M}[T] = 0, B_{k,m}^{U\to M}[t] \ge 0, \forall k, m, t \in \mathcal{T}_2, \tag{23v}$$

$$B_{k,m}^{U\to K}[1] = B_{k,m}^{U\to K}[2] = 0, B_{k,m}^{U\to K}[t] \ge 0, \forall k, m, t \in \mathcal{T}_3. \tag{23w}$$

C_{max} is the maximum capacity of the MEC device and $\mathcal{T}_1$ is defined as $\mathcal{T}_1 = \{1, \dots, T-2\}$. In problem (23), the constraints (23b) - (23d) are connection scheduling constraints. The constraints (23e) and (23f) represent the transmission power limits of the IoRT devices and the UAVs, where $P_{max}^{D\to U}$ and $P_{max}^{U\to M}$ represent the maximum transmission powers of the IoRT devices and the UAVs, respectively. (23g) indicates that the UAV should come back to its initial location at the end of time period while (23h) is constraint on the speed of the UAV. (23i) and (23j) are coverage area constraint and collision avoidance constraint of the UAVs, respectively. The constraint (23k) ensures that the total amount of data transmitted to the MEC device does not exceed the capacity of the MEC device. (23l) and (23m) are information-causality constraints, while the constraints (23n)–(23p) ensure that the data of the IoRT devices has been processed and output has been received. (23q) is the bandwidth constraint. The constraints (23r)–(23w) ensure the non-negativeness of the optimization variables and also indicate that the IoRT devices should not offload in the last two slots, while the UAV should not offload the data received from the IoRT devices in the first and last slots as well as not transmit the output data to the IoRT devices in the first two slots. It is to be noted that both the energy and throughput are represented as unit-less values. In other words, we are performing normalization by dividing the throughput and the energy consumption with their respective unit values. This is done to enable the formulation of multi-objective optimization problem involving both the parameters. ζ is a penalty coefficient to the throughput, used to mitigate the magnitude difference between the absolute values of energy and throughput.

Intractability: Solving the problem (23) is challenging due to the following reasons. Firstly, the objective function is non-convex. Secondly, in (23d), the connection scheduling variable $c_{k,m}[t]$ is a binary variable, which is an integer constraint. Thirdly, the constraints (23j) and (23k) are non-convex constraints. Finally, there exist non-linear couplings between the variables $l_{k,m}^{D\to U}[t]$, $B_{k,m}^{D\to U}[t]$ and $l_{k,m}^{U\to M}[t], B_{k,m}^{U\to M}[t]$ and $l_{k,m}^{U\to K}[t], B_{k,m}^{U\to K}[t]$, and these variables are strongly coupled with the trajectories of the UAVs. It can be observed that the problem (23) is a complicated Mixed Integer Non Linear Programming (MINLP) problem. Therefore, we cannot use standard convex optimization techniques to solve the problem (23).

4. Solution design

To make the optimization problem (23) tractable, we relax the binary variable in (23d) into continuous variables. It yields the following problem:

$$\min_{\{\mathbf{C},\mathbf{U},\mathbf{P}^{D\to U},\mathbf{P}^{U\to M},\mathbf{B},\mathbf{L}\}} E-\zeta\sum_{m=1}^{M}\sum_{k=1}^{K}R_{k,m}, \tag{24a}$$

$$s.t. \quad (23b), (23c), (23e)–(23w), \tag{24b}$$

$$c_{k,m}[t]\in[0,1], \forall k,m,t. \tag{24c}$$

In general, such a relaxation implies that the objective value of problem (24) serves as an upper bound for the objective value of problem (23). Despite being relaxed, the problem (24) is still a non-convex optimization problem because of the constraints (23j) and (23k).

We propose a BCD based iterative algorithm for solving the problem (23), by dividing it into five sub-problems. In the first sub-problem, the IoRT devices connection scheduling ($\mathbf{C}$) is optimized for the given UAV trajectories, ($\mathbf{U}$), the transmission power of IoRT devices ($\mathbf{P}^{D\to U}$), the transmission power of UAVs ($\mathbf{P}^{U\to M}$), the bandwidth allocation ($\mathbf{B}$) and the bit transmission scheduling ($\mathbf{L}$). In the second sub-problem, the transmission power of IoRT devices ($\mathbf{P}^{D\to U}$) and the transmission power of UAVs ($\mathbf{P}^{U\to M}$) are optimized fixing all the other variables. Similarly, in the third and fourth sub-problems, the bit transmission scheduling ($\mathbf{L}$) and the bandwidth allocation ($\mathbf{B}$) are optimized, respectively. Finally, the UAV trajectories are optimized.

4.1. IoRT devices connection scheduling optimization

For the given UAV trajectories, transmission powers, bandwidth allocation and bit transmission scheduling $\{\mathbf{U},\mathbf{P}^{D\to U},\mathbf{P}^{U\to M},\mathbf{B},\mathbf{L}\}$, the first sub-problem to optimize the IoRT devices connection scheduling ($\mathbf{C}$) can be formulated as

$$\begin{aligned}&\min_{\mathbf{C}}\sum_{m=1}^{M}\sum_{k=1}^{K}-R_{k,m}+\\&c_{k,m}[t]\sum_{m=1}^{M}\sum_{k=1}^{K}\sum_{t=1}^{T}\left(w_1E_{k,m}^{D\to U}[t]+w_2E_{k,m}^{U\to K}[t]\right),\\&s.t. \quad (23b), (23c), (23i), (23k), (23p), (24c)\end{aligned} \tag{25}$$

It can be observed that the problem (25) is a standard Linear Programming (LP) problem. It can be solved by using the optimization toolbox CVX [37].

4.2. Power control optimization

For the given IoRT devices connection scheduling, UAV trajectories, bandwidth allocation and bit transmission scheduling $\{\mathbf{C},\mathbf{U},\mathbf{B},\mathbf{L}\}$, the second sub-problem to optimize the transmission powers ($\mathbf{P}^{D\to U},\mathbf{P}^{U\to M}$) can be formulated as

$$\begin{aligned}&\min_{\{\mathbf{P}^{D\to U},\mathbf{P}^{U\to M}\}} -\sum_{m=1}^{M}\sum_{k=1}^{K}R_{k,m},\\&s.t. \quad (23e), (23f), (23k), (24c)\end{aligned} \tag{26}$$

The problem (26) is a non-convex optimization problem due to the non-convex objective function $-R_{k,m}$ and non-convex constraint (23k). We develop the solution to the subproblem (26) on similar lines with the method followed in [3]. We apply variable substitution and then transform the subproblem into a convex optimization problem using Successive Convex Approximation (SCA). Since $P_{k,m}^{D\to U}[t], P_m^{U\to M}[t] > 0, \forall k,m,t$, we introduce the auxiliary variables $\alpha_{k,m}[t]$ and $\beta_m[t]$, where $P_{k,m}^{D\to U}[t] \triangleq e^{\alpha_{k,m}[t]}$ and $P_m^{U\to M}[t] \triangleq e^{\beta_m[t]}$. Now, by substituting (5) and (7) in (8), the throughput $R_{k,m}[t]$ can be written as

$$\begin{aligned}R_{k,m}[t]&\\&=B[log_2(\sigma^2+e^{\alpha_{k,m}[t]}h_{k,m}^{D\to U}[t]+e^{\beta_m[t]}h_m^{U\to M}[t]\\&+e^{\alpha_{k,m}[t]+\beta_m[t]}h_{k,m}^{D\to U}[t]h_m^{U\to M}[t])\\&-log_2(\sigma^2(\sigma^2+e^{\alpha_{k,m}[t]}h_{k,m}^{D\to U}[t]+e^{\beta_m}h_m^{U\to M}[t]))]\\&\triangleq B(\Phi_1-\Phi_2)\end{aligned} \tag{27}$$

where $\Phi_1 = log_2(\sigma^2+e^{\alpha_{k,m}[t]}h_{k,m}^{D\to U}[t]+e^{\beta_m[t]}h_m^{U\to M}[t]+e^{\alpha_{k,m}[t]+\beta_m[t]}h_{k,m}^{D\to U}[t]h_m^{U\to M}[t])$ and $\Phi_2 = log_2(\sigma^2(\sigma^2+e^{\alpha_{k,m}[t]}h_{k,m}^{D\to U}[t]+e^{\beta_m[t]}h_m^{U\to M}[t]))$. As both Φ_1 and Φ_2 are convex functions, $R_{k,m}[t]$ is difference of convex programming problem. We can express it as:

$$\begin{aligned}&\min_{\{\alpha,\beta\}} -\sum_{m=1}^{M}\sum_{k=1}^{K}R_{k,m},\\&s.t. \quad (23k), (24c)\\&0\le e^{\alpha_{k,m}[t]}\le P_{max}^{D\to U}[t], \forall k,m,t,\\&0\le e^{\beta_m[t]}\le P_{max}^{U\to M}[t], \forall m,t,\end{aligned} \tag{28}$$

The problem (28) is non-convex optimization problem due to the non-convex objective function $-R_{k,m}$. To make the problem (28) tractable, we apply SCA to approximate Φ_1 to a linear function $\tilde{\Phi}_1$ using first-order Taylor expansion in each iteration. Let $\tilde{R}_{k,m}[t] \triangleq B(\Phi_2-\tilde{\Phi}_1)$; it is a convex function. We define $\mathbf{P}^{D\to U^r} = \{P_{k,m}^{D\to U^r}[t], \forall k,m,t\}$ and $\mathbf{P}^{U\to M^r} = \{P_m^{U\to M^r}[t], \forall k,m,t\}$, which represent the transmission power value of IoRT devices to the UAVs and the transmission power values of UAVs to the MEC device in the rth iteration, respectively. Then $\boldsymbol{\alpha}^r = \{\alpha_{k,m}^r[t], \forall k,m,t\}$ and $\boldsymbol{\beta}^r = \{\beta_m^r[t], \forall k,m,t\}$ represent the variable substitution values given by $\mathbf{P}^{D\to U^r}$ and $\mathbf{P}^{U\to M^r}$ in the rth iteration, respectively. Therefore, we can obtain the lower bound $\tilde{\Phi}_1$ of Φ_1 using SCA, as below:

$$\begin{aligned}\Phi_1\ge\tilde{\Phi}_1&=log_2(e^{\alpha_{k,m}^r[t]+\beta_m^r[t]}h_{k,m}^{D\to U}[t]h_m^{U\to M}[t])+\\&\frac{1}{ln(2)}[(\alpha_{k,m}[t]-\alpha_{k,m}^r[t])+(\beta_m[t]-\beta_m^r[t])]\end{aligned} \tag{29}$$

Then the throughput is given by $\tilde{R}_{k,m} = \frac{1}{T}\sum_{t=1}^{T}c_{k,m}[t]\tilde{R}_{k,m}[t]$. The problem (28) can be approximated as below:

$$\begin{aligned}&\min_{\{\alpha,\beta\}}\sum_{m=1}^{M}\sum_{k=1}^{K}\tilde{R}_{k,m},\\&s.t. \quad (24c),\\&\sum_{t=1}^{T}\sum_{m=1}^{M}\sum_{k=1}^{K}c_{k,m}[t]\tilde{R}_{k,m}[t]\le C_{max}\\&0\le e^{\alpha_{k,m}[t]}\le P_{max}^{D\to U}[t], \forall k,m,t,\\&0\le e^{\beta_m[t]}\le P_{max}^{U\to M}[t], \forall m,t,\end{aligned} \tag{30}$$

As the problem (30) is a convex optimization problem, it can be solved using the CVX toolbox [37].

4.3. Bit transmission scheduling optimization

For the given IoRT devices connection scheduling, UAV trajectories, transmission powers, and bandwidth allocation $\{\mathbf{C},\mathbf{U},\mathbf{P}^{D\to U},\mathbf{P}^{U\to M},\mathbf{B}\}$, the third sub-problem to optimize the bit transmission scheduling $(\mathbf{L})$ can be formulated as

$$\min_{\mathbf{L}} \sum_{m=1}^{M}\sum_{k=1}^{K}\sum_{t=1}^{T}\Big(w_1 c_{k,m}[t]E_{k,m}^{D\to U}[t] + w_2(E_{k,m}^{U\to M}[t] + c_{k,m}[t]E_{k,m}^{U\to K}[t])\Big)$$
$$s.t.\quad (23l)\text{–}(23p),\ (23r)\text{–}(23t) \tag{31}$$

As the UAV trajectories are fixed, the time-dependent channels and $h_{k,m}^{D\to U}[t]$ and $h_{m}^{U\to M}[t]$ are also known. Besides, the non-linear couplings between the variables $l_{k,m}^{D\to U}[t]$, $B_{k,m}^{D\to U}[t]$ and $l_{k,m}^{U\to M}[t]$, $B_{k,m}^{U\to M}[t]$ and $l_{k,m}^{U\to K}[t]$, $B_{k,m}^{U\to K}[t]$ no longer exist. As the objective function and constraints are convex, the resource scheduling problem (31) is convex. Therefore, we can use CVX to solve it.

4.4. Bandwidth allocation optimization

For the given IoRT devices connection scheduling, UAV trajectories, transmission powers and bit transmission scheduling $\{\mathbf{C},\mathbf{U},\mathbf{P}^{D\to U},\mathbf{P}^{U\to M},\mathbf{L}\}$, the fourth sub-problem to optimize the bandwidth allocation $(\mathbf{B})$ can be formulated as

$$\min_{\mathbf{B}} \sum_{m=1}^{M}\sum_{k=1}^{K}\sum_{t=1}^{T}\Big(w_1 c_{k,m}[t]E_{k,m}^{D\to U}[t] + w_2(E_{k,m}^{U\to M}[t] + c_{k,m}[t]E_{k,m}^{U\to K}[t])\Big)$$
$$s.t.\quad (23q),\ (23u)\text{–}(23w) \tag{32}$$

It can be observed that the problem (32) is convex with a convex objective function and convex constraints. We leverage the Lagrange duality method to solve the problem (32). The corresponding optimal solution is given in Theorem 1.

Theorem 1. *The optimal solution for problem (32) is given by the Eqs. (33)–(35).*

Proof. See Appendix. □

$$B_{k,m}^{D\to U*}[t] = \begin{cases} \dfrac{\frac{\ln 2}{2} l_{k,m}^{D\to U}[t]}{\delta W_0\left[\frac{\ln 2}{2}\left(\frac{\phi_{k,m,t}}{w_1}h_{k,m}^{D\to U}[t]l_{k,m}^{D\to U}[t]\right)^{\frac{1}{2}}\right]}, t\in\mathcal{T}_1,\\ 0, t = T-1 \text{ or } T,\end{cases} \tag{33}$$

$$B_{k,m}^{U\to M*}[t] = \begin{cases} \dfrac{\frac{\ln 2}{2} l_{k,m}^{U\to M}[t]}{\delta W_0\left[\frac{\ln 2}{2}\left(\frac{\phi_{k,m,t}}{w_2}h_{k,m}^{U\to M}[t]l_{k,m}^{U\to M}[t]\right)^{\frac{1}{2}}\right]}, t\in\mathcal{T}_2,\\ 0, t = 1 \text{ or } T,\end{cases} \tag{34}$$

$$B_{k,m}^{U\to K*}[t] = \begin{cases} \dfrac{\frac{\ln 2}{2} l_{k,m}^{U\to K}[t]}{\delta W_0\left[\frac{\ln 2}{2}\left(\frac{\phi_{k,m,t}}{w_2}h_{k,m}^{D\to U}[t]l_{k,m}^{U\to K}[t]\right)^{\frac{1}{2}}\right]}, t\in\mathcal{T}_3,\\ 0, t = 1 \text{ or } 2,\end{cases} \tag{35}$$

where $\phi_{k,m,t} = \frac{\rho^*_{k,m,t}}{\delta^2\sigma^2\ln(2)}$ with $\rho^* = \{\rho^*_{k,m,t}, \forall k,m,t\}$ being the optimal Lagrange multipliers (dual variables). $W_0(x)$ is the principal branch of the Lambert W function defined as the solution of $W_0(x)e^{W_0(x)} = x$ [38].

It can be observed that, to find out the optimal bandwidth allocation $\mathbf{B}^*$, we need to obtain the optimal values of the Lagrange multipliers, ρ^*. We adopt a subgradient-based algorithm to obtain the optimal dual variables. The subgradient method of dual variables is

$$\rho_{k,m,t}^{(j+1)} = \left[\rho_{k,m,t}^{(j)} - \theta_4^{(j)}\Big(B_{k,m}^{D\to U*}[t] + B_{k,m}^{U\to M*}[t] + B_{k,m}^{U\to K*}[t] - B\Big)\right]^+, \forall k,m,t, \tag{36}$$

where $\theta_4^{(j)}$ denotes the iterative step for obtaining the dual variables in ρ at the jth iteration. Also $\{B_{k,m}^{D\to U*}[t]\}, \{B_{k,m}^{U\to M*}[t]\}, \{B_{k,m}^{U\to K*}[t]\}$ are the values obtained at the jth iteration using the Eqs. (33)–(35). The convergence to the optimal value is guaranteed by the subgradient with a small error range [39].

4.5. UAV trajectory optimization

For the given IoRT devices connection scheduling, transmission powers, bandwidth allocation and bit transmission scheduling $\{\mathbf{C},\mathbf{P}^{D\to U},\mathbf{P}^{U\to M},\mathbf{B},\mathbf{L}\}$, the fifth sub-problem to optimize the UAV trajectories $(\mathbf{U})$ can be formulated as

$$\min_{\mathbf{U}} \quad E - \zeta\sum_{m=1}^{M}\sum_{k=1}^{K} R_{k,m}, \tag{37}$$
$$s.t. (23g)\text{–}(23j),\ (23k),\ (24c)$$

It can be seen that the energy consumption E is convex with respect to the trajectory $\mathbf{U}$. However, the problem (37) is non-convex optimization problem as we cannot determine the concavity or convexity of $-R_{k,m}[t]$ with respect to $\mathbf{u}_m[t]$ and the constraints (23j) and (23k) are non-convex constraints.

We use the SCA technique for the trajectory optimization and approximate the original function by a more manageable function at a given local point, in each iteration. We define $\mathbf{u}^r = \{\mathbf{u}_m^r[t], \forall m,t\}$ as the UAV trajectory in the rth iteration. As the constraint (23j) is a convex function with respect to $\mathbf{u}_m[t]$ and $\mathbf{u}_j[t]$, we can apply the first-order Taylor expansion at any given $\mathbf{u}_m^r[t]$ and $\mathbf{u}_j^r[t]$ to obtain its lower bound. The Taylor expansion is presented in the equation below

$$\begin{aligned} R_{k,m}[t] \geq \check{R}_{k,m}[t] = &B log_2\left(1+\frac{X}{Y}\right) - \frac{BX}{ln(2)(Y+X)Y}\\ &\left(P_{k,m}^{D\to U}[t](\mathbf{u}_m^r[t]-\mathbf{w}_M) - P_m^{U\to M}[t](\mathbf{u}_m^r[t]-\mathbf{w}_k)\right)\\ &.\left(\mathbf{u}_m[t]-\mathbf{u}_m^r[t]\right)',\end{aligned} \tag{38}$$

$$\begin{aligned}\|\mathbf{u}_m[t]-\mathbf{u}_j[t]\|^2 \geq -\|\mathbf{u}_m^r[t]-\mathbf{u}_j^r[t]\|^2 + 2(\mathbf{u}_m^r[t]-\mathbf{u}_j^r[t])^{\mathrm{T}}\\ \times(\mathbf{u}_m[t]-\mathbf{u}_j[t])\forall m, j\neq m, t\in\mathcal{T}.\end{aligned} \tag{39}$$

We also transform the problem (37) by applying SCA. We apply first order Taylor expansion approximate $R_{k,m}[t]$ to a linear function $\check{R}_{k,m}[t]$ at any point iteratively, where $\check{R}_{k,m}[t]$ is the lower bound of $R_{k,m}[t]$. The Taylor expansion of $R_{k,m}[t]$ at the rth iteration is presented in Eq. (38), where,

$$\begin{aligned} X =&\frac{P_{k,m}^{D\to U}[t]P_m^{U\to M}[t]h_0}{\sigma^2},\\ Y =&P_{k,m}^{D\to U}[t]\left((H-H_m)^2 + \|\mathbf{u}_m^r[t]-\mathbf{w}_M\|^2\right)\\ &+ P_m^{U\to M}[t]\left(H^2 + \|\mathbf{u}_m^r[t]-\mathbf{w}_k\|^2\right)\end{aligned}$$

The throughput is denoted by $\check{R}_{k,m} = \frac{1}{T}\sum_{t=1}^{T} c_{k,m}[t]\check{R}_{k,m}[t]$ Now, the problem (37) can be reformulated as below

$$\begin{aligned} \min_{\mathbf{U}} \quad & E - \zeta\sum_{m=1}^{M}\sum_{k=1}^{K}\check{R}_{k,m},\\ s.t.& (23g)\text{–}(23i),\ (24c)\\ &-\|\mathbf{u}_m^r[t]-\mathbf{u}_j^r[t]\|^2 + 2(\mathbf{u}_m^r[t]-\mathbf{u}_j^r[t])^{\mathrm{T}}\times(\mathbf{u}_m[t]-\mathbf{u}_j[t])\\ &\qquad\geq d_{min}^2 \forall m,t,j\neq m,\\ &\sum_{k=1}^{K} L_k(1+O_k) \leq \sum_{t=1}^{T}\sum_{m=1}^{M}\sum_{k=1}^{K} c_{k,m}[t]\check{R}_{k,m}[t]\\ &\qquad\leq C_{max}, \forall k,m,t,\end{aligned} \tag{40}$$

It can be seen that the problem (40) is a convex optimization problem and can be solved using the CVX toolbox [37].

4.6. Algorithm

In this section we propose an overall iterative algorithm to obtain the results of joint optimization of resource allocation and multi-UAV trajectory using BCD. Specifically, we perform the optimization of the IoRT devices connection scheduling ($\mathbf{C}$), the transmission power of IoRT devices ($\mathbf{P}^{D\rightarrow U}$) and the transmission power of UAVs ($\mathbf{P}^{U\rightarrow M}$), the bit transmission scheduling ($\mathbf{L}$), the bandwidth allocation ($\mathbf{B}$) and the UAV trajectories ($\mathbf{U}$) alternately in each iteration. Let us represent the objective function of the original problem i.e., the problem (23) be represented by $\boldsymbol{\mathcal{O}}$. We propose the Algorithm 1 to solve the original problem (23) for obtaining the solution $\{\mathbf{C}^{*}, \mathbf{P}^{D\rightarrow U*}, \mathbf{P}^{U\rightarrow M*}, \mathbf{L}^{*}, \mathbf{B}^{*}, \mathbf{U}^{*}\}$.[2] The algorithm solves the five sub problems in five stages. In each stage, except the variables to be determined in the subproblem under consideration, all the other variables are kept constant. The algorithm stops when convergence is achieved i.e., when the change in the objective value of the algorithm between two consecutive iterations falls below the threshold value ϵ. As we use CVX to solve the sub-problems, the computational complexity is acceptable, in general [7]. To perform numerical simulations, we used the MOSEK solver supported by the CVX which employs the interior-point method. The complexity of interior-point method is given by $\mathcal{O}(\kappa^{\frac{1}{2}}(\kappa+\upsilon)^2)$ [40,41], where κ represents the number of inequality constraints, υ represents the number of variables. Hence, the complexity of the problems (25), (30), (31) can be calculated as $\mathcal{O}((KMT)^{3.5})$ and the complexity of the problem (40) can be calculated as $\mathcal{O}(K^{1.5}(MT)^{3.5})$. For the problem (32), each iteration takes $\mathcal{O}(KMT)$ time and it is experimentally observed that the problem (32) converges in a few iterations. Therefore, the overall time complexity of Algorithm 1 can be given as $\mathcal{O}(3(KMT)^{3.5} + K^{1.5}(MT)^{3.5} + KMT)$.

Algorithm 1: Five-stage iterative algorithm for solving problem (23)

Let $r = 0$, initialize $\mathbf{C}^0, \mathbf{P}^{D\rightarrow U^0}, \mathbf{P}^{U\rightarrow M^0}, \mathbf{L}^0, \mathbf{B}^0, \mathbf{U}^0$ `// r is the iteration number`
Calculate $\mathcal{O}^0$, the objective of the problem (23) using $\mathbf{C}^0, \mathbf{P}^{D\rightarrow U^0}, \mathbf{P}^{U\rightarrow M^0}, \mathbf{L}^0, \mathbf{B}^0, \mathbf{U}^0$
repeat
  Given $\mathbf{C}^r, \mathbf{P}^{D\rightarrow U^r}, \mathbf{P}^{U\rightarrow M^r}, \mathbf{L}^r, \mathbf{B}^r, \mathbf{U}^r$, solve the problem (25). The solution obtained is represented by $\mathbf{C}^{r+1}$
  Given $\mathbf{C}^{r+1}, \mathbf{P}^{D\rightarrow U^r}, \mathbf{P}^{U\rightarrow M^r}, \mathbf{L}^r, \mathbf{B}^r, \mathbf{U}^r$, solve the problem (30). The solution obtained is represented by $\mathbf{P}^{D\rightarrow U^{r+1}}, \mathbf{P}^{U\rightarrow M^{r+1}}$
  Given $\mathbf{C}^{r+1}, \mathbf{P}^{D\rightarrow U^{r+1}}, \mathbf{P}^{U\rightarrow M^{r+1}}, \mathbf{L}^r, \mathbf{B}^r, \mathbf{U}^r$, solve the problem (31). The solution obtained is represented by $\mathbf{L}^{r+1}$
  Given $\mathbf{C}^{r+1}, \mathbf{P}^{D\rightarrow U^{r+1}}, \mathbf{P}^{U\rightarrow M^{r+1}}, \mathbf{L}^{r+1}, \mathbf{B}^r, \mathbf{U}^r$, solve the problem (32). The solution obtained is represented by $\mathbf{B}^{r+1}$
  Given $\mathbf{C}^{r+1}, \mathbf{P}^{D\rightarrow U^{r+1}}, \mathbf{P}^{U\rightarrow M^{r+1}}, \mathbf{L}^{r+1}, \mathbf{B}^{r+1}, \mathbf{U}^r$, solve the problem (40). The solution obtained is represented by $\mathbf{U}^{r+1}$
  Calculate $\mathcal{O}^{r+1}$ using $\mathbf{C}^{r+1}, \mathbf{P}^{D\rightarrow U^{r+1}}, \mathbf{P}^{U\rightarrow M^{r+1}}, \mathbf{L}^{r+1}, \mathbf{B}^{r+1}, \mathbf{U}^{r+1}$ Update $r = r + 1$;
until *convergence i.e.,* $|\mathcal{O}^r - \mathcal{O}^{r+1}| < \epsilon$
At convergence, $\mathbf{C}^*, \mathbf{P}^{D\rightarrow U^*}, \mathbf{P}^{U\rightarrow M^*}, \mathbf{L}^*, \mathbf{B}^*, \mathbf{U}^*$ represent the solution

5. Numerical simulation

In this section, we present the numerical simulation results to evaluate our proposed algorithm. We adopted the simulation parameters from [3,4], and [7]. We chose the total bandwidth available to each UAV, B to be 30 MHz. The length of entire time duration $\mathscr{T}$ is chosen as 10 s. The number of time slots T is 20 and hence each time slot is of the length 0.5 s. The number of UAVs (M) and the number of IoRT devices (K) are 3 and 15, respectively, unless specified otherwise. The IoRT devices are randomly spread over a circular area of the radius 300 m. The noise power spectral density is taken as −60 dBm/Hz, while the channel gain at a reference distance of 1 m is −30 dB. The heights of the UAVs (H) and of the antenna of the MEC device (H_m) are 10 m and 20 m, respectively. The maximum speed of the UAV is 10 m/s, while the mass of the UAV (Q) is 9.65 kg. The minimum safety distance between any two UAVs, d_{min} is taken as 51 m. The weights w_1 and w_2 are chosen to be 0.2 and 0.8, respectively, unless specified otherwise. The maximum transmission power of the IoRT devices ($P_{max}^{D\rightarrow U}[t], t \in \mathcal{T}$) is 1 W, while that of the UAVs ($P_{max}^{U\rightarrow M}[t], t \in \mathcal{T}$) is 50 W. Unless specified otherwise, the task-input data size at each IoRT device is chosen randomly between 50 Mb and 300 Mb. The value of task size ratio of output data to input data ($O_k, k \in \mathcal{K}$) is taken as 0.8.

To run the simulations, we used MATLAB R2022a and CVX. We used 64-bit Intel i7 system of 8 cores with CPU speed of 3.4 GHz.

Figs. 2 and 3 illustrate the convergence of the proposed algorithm. For these two graphs, the data size at each IoRT device is fixed at 100 Mb. It can be seen that both the energy consumption and throughput values stabilize within 8 iterations. The two graphs combined is shown in Fig. 4, depicting trade off between the energy consumption and system throughput values. The trends of system throughput and energy consumption are plotted varying the value of ζ, the weight to offset the difference in magnitude of system throughput and energy consumption, from 5 to 25. It is observed that the lower value of ζ leads to higher value of system throughput and lower value of energy consumption. Therefore, we use the value of $\zeta = 1$ for our simulations. We also plotted a graph Fig. 5, showing the convergence of energy consumption value, varying the data sizes at each IoRT device. For Fig. 5, the data size at each IoRT device is chosen randomly between 50 Mb and 550 Mb as shown in the legend. It can be seen that, even with higher data size at each IoRT device, the weighted energy consumption value converges within 15 iterations. Fig. 6 illustrates the trajectories of the three UAVs computed using the proposed solution. It can be seen that the three UAVs cover the IoRT devices without overlapping each other's coverage areas and maintaining the minimum safety distance between them at all times.

We plotted the average number of bits transmitted by the IoRT devices to the UAVs in each time slot in Fig. 7. Similarly, the average number of bits transmitted by the UAVs to the MEC device in each time slot is presented in Fig. 8. Fig. 9 shows the average number of bits the UAVs transmit in each time slot to the IoRT device. It can be seen that the IoRT devices try to transmit maximum number of bits as early as possible. The UAVs then transmit the bits to the MEC device over the entire duration in a semi-uniform fashion. After getting the results back from the MEC device, the UAVs transmit the data back to IoRT devices. However it can be seen that most of the results data is transmitted by the UAVs to IoRT devices in the later time slots. As the UAVs are in continuous motion, the UAVs have to wait till the desired IoRT device comes into its range. It can inferred that the entire process is handled in three phases. In the first few time slots, the UAVs are collecting the data. In the next few time slots, the UAVs send the data to the MEC device and get the results back. In the last few time slots, the results are return back to the IoRT devices. The trajectories of UAVs are optimized accordingly. Hence we see the transmission from IoRT devices to the UAVs prominently in the first few time slots, and transmission from the UAVs to the IoRT devices prominently in the last few time slots.

Fig. 10 illustrates that throughput increases both with increase in maximum transmit powers of IoRT devices and that of UAVs. As the maximum transmit power increases, more data can be transmitted and hence the average system throughput increases.

Fig. 11 shows the average transmit power of IoRT devices over time. It can be noticed that the transmit powers of IoRT devices is always

[2] The proposed algorithm is not optimal theoretically due to the non-convexity of the problem. However, its performance gain is verified by the numerical simulations.

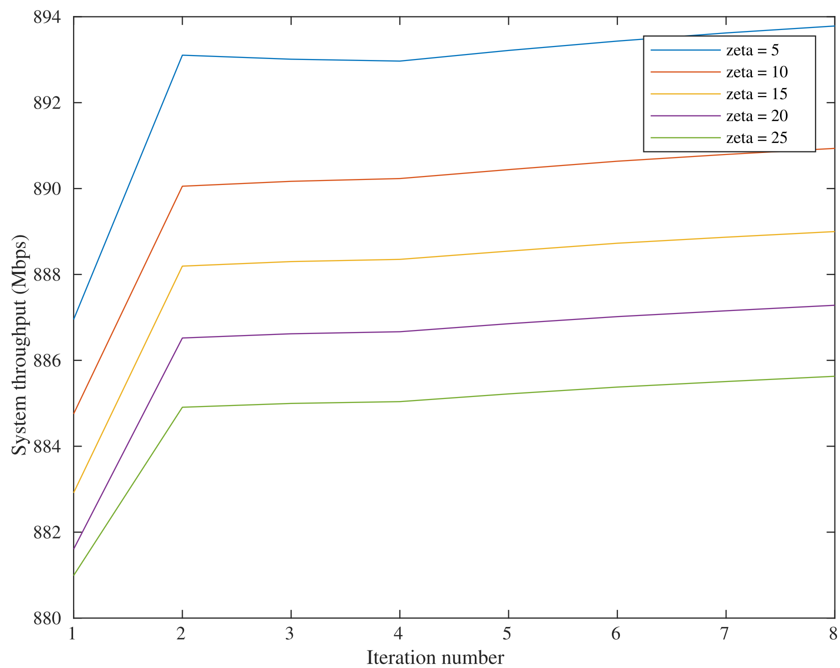

Fig. 2. System throughput vs number of iterations.

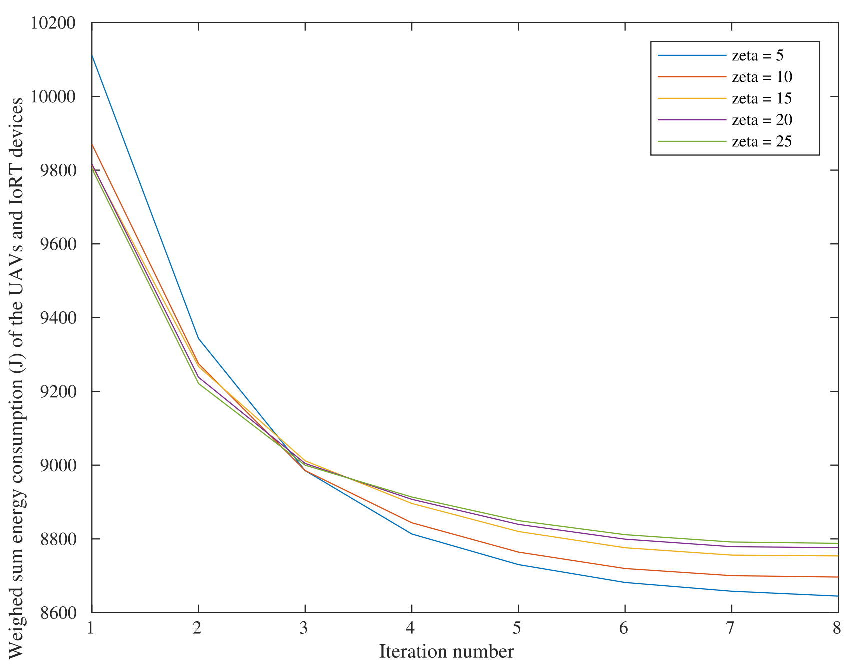

Fig. 3. Energy consumption vs number of iterations.

between 0.2 W and 0.3 W. This is significant improvement over [3], where the devices are observed to be transmitting with maximum power (i.e., 1 W) all the time. The improvement is because of the joint optimization of the energy consumption and system throughput while [3] optimizes only the system throughput. Fig. 12 shows the weighted sum energy consumption while varying the parameter w_2 for both proposed algorithm and equal bandwidth allocation method. It can be noted that the equal bandwidth allocation performs similar to the proposed algorithm, while the proposed solution performs slightly better when the value of w_2 is greater than 0.6 i.e., when more weightage is given for the energy consumption by the UAVs compared to the weightage given to the energy consumption by the IoRT devices. It implies that the energy consumed by the UAVs is significantly higher compared to the energy consumed by the IoRT

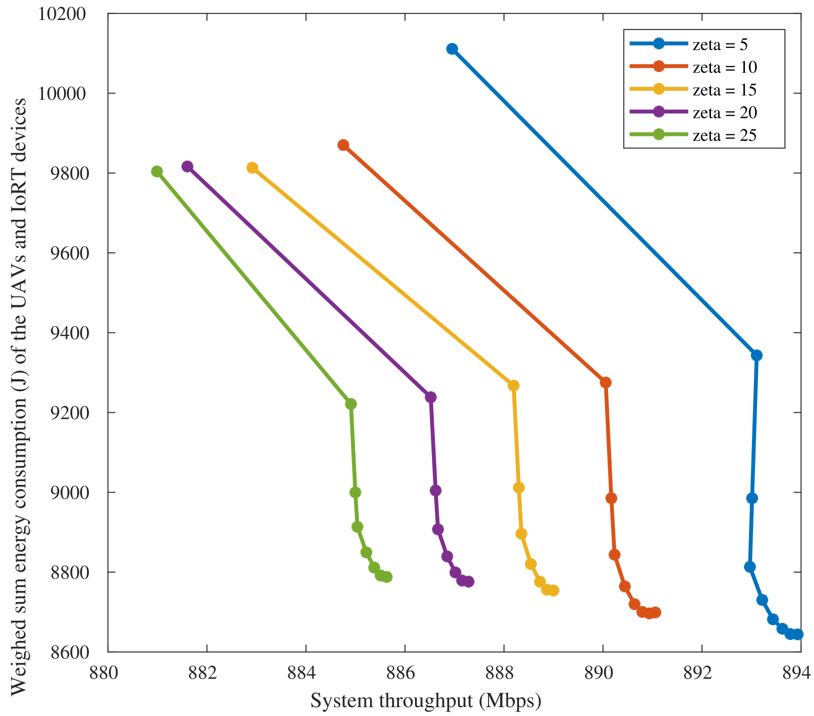

Fig. 4. Trade off between energy consumption vs system throughput.

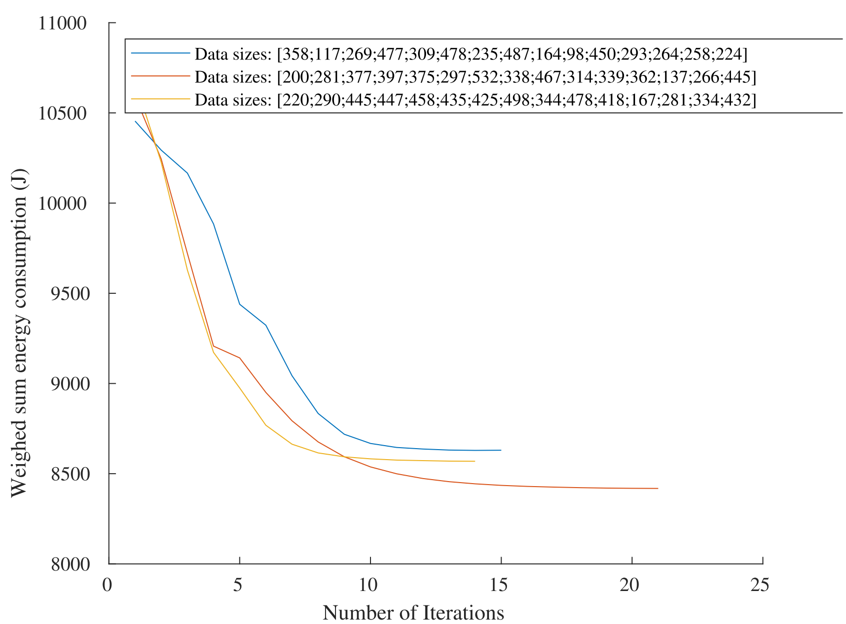

Fig. 5. Energy consumption vs number of iterations for varying data sizes.

devices. In other words, it can be inferred that flying the UAV takes more energy that transmission of the data.

Fig. 13 compares the energy consumption for the proposed solution, circular trajectory method and static UAVs case in which the UAVs are static at their respective locations, for varying number of IoRT devices. For Fig. 13, the value of w_2 is fixed as 0.5. It can be seen that the proposed solution always consumes lower energy compared to the circular trajectory method and static UAVs method. When the number of IoRT devices is 10, the energy consumption for the proposed solution, circular trajectory method and static UAVs method are observed to be 10.1 KJ, 10.67 KJ, and 14.04 KJ, respectively. When the number of IoRT devices is 50, the energy consumption for the proposed solution, circular trajectory method and static UAVs method are observed respectively to be 9.4 KJ, 14.9 KJ, and 18.3 KJ. In other words, the proposed solution achieves around 37% better performance compared to circular trajectory method and 48.6% better performance compared to static UAVs method. Two observations are made in this experiment. First, UAV flight energy dominates the energy required for transmission. Second, when the number of IoRT devices are less and equal weightage is assigned to the energy consumption of the UAV and energy consumption of the IoRT devices, the algorithm tries to optimize the trajectory in such a way that the UAV visits the IoRT devices

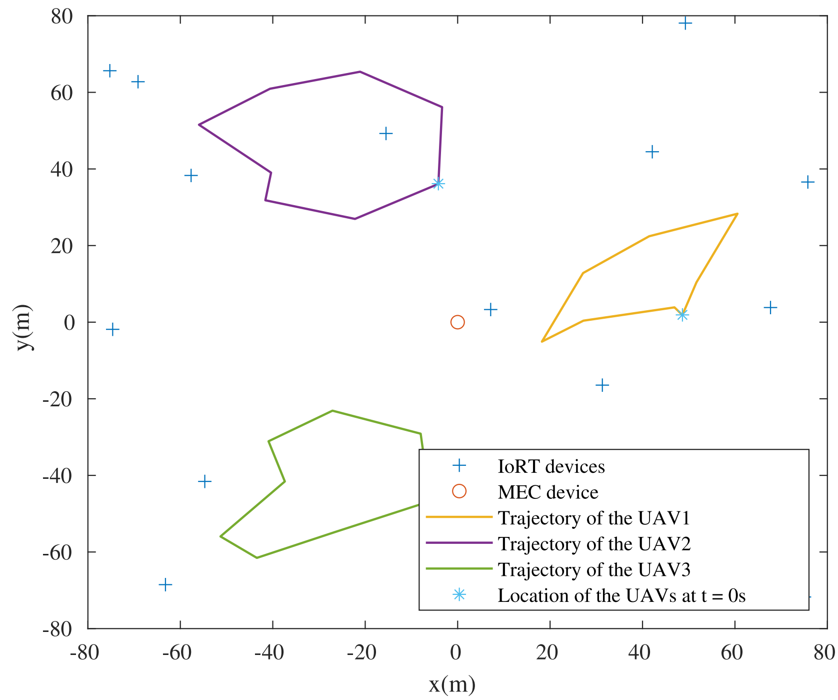

Fig. 6. Trajectory design for M = 3 and K = 15.

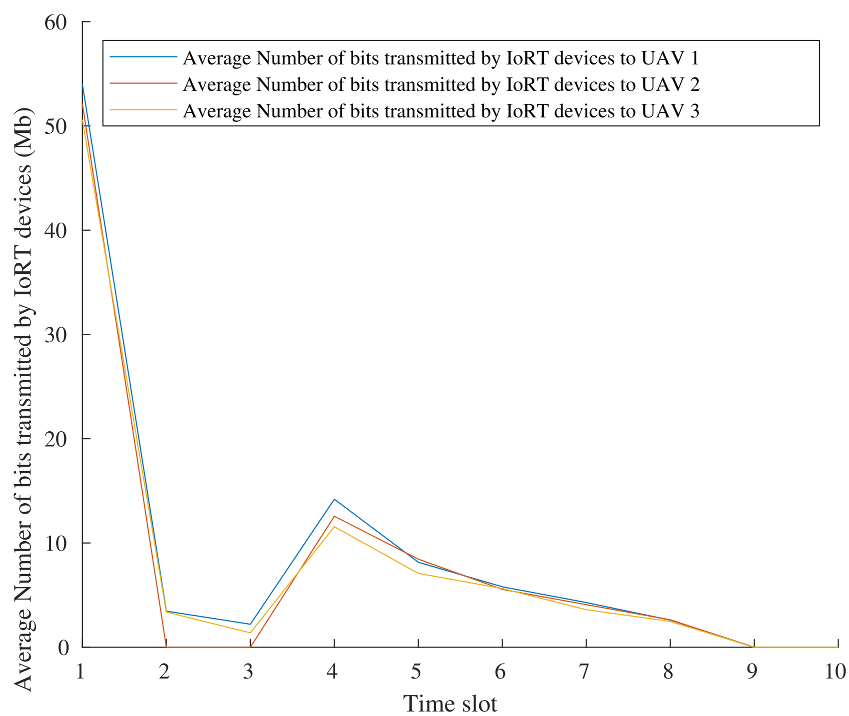

Fig. 7. Average Number of bits transmitted by IoRT devices (Mb).

by going as near to them as possible. This increases the UAV flight energy consumption and hence the total weighted energy consumption. However, when the number of IoRT devices increases, the UAV does not visit the proximity of each IoRT device. Hence, the UAV flight energy consumption is reduced and hence the total weighted energy consumption.

In Fig. 14, we plotted the weighted energy consumption values, varying the number of devices, for three different placements of UAV — on the ground, on the UAV and on the (LEO) satellite. The first placement is the proposed solution, wherein the UAV acts a relay between IoRT devices and the MEC device installed on the ground nearby. In the second placement i.e., placing MEC in the UAV, the computations are carried out at the MEC devices carried by the UAV. In the third placement, MEC is installed in the satellite and UAV is used to relay the data collected from the IoRT devices to the satellite. For this graph, we also factored in the energy need for the UAV to

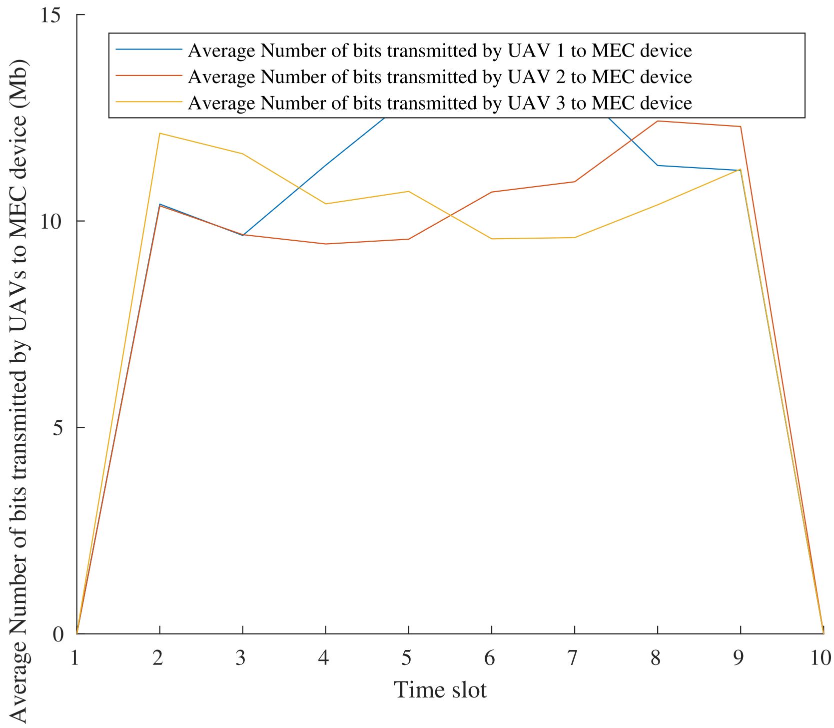

Fig. 8. Average Number of bits transmitted by UAVs to MEC device (Mb).

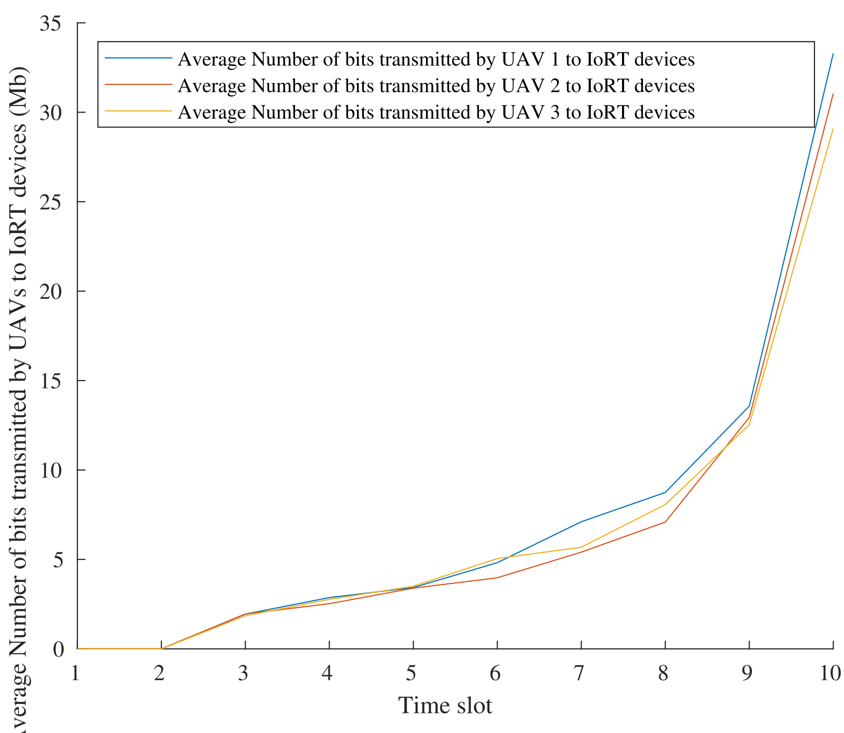

Fig. 9. Average Number of bits transmitted by UAVs to IoRT devices (Mb).

travel to the charging station. When the number of devices K is 5, the three placements — MEC on ground, MEC at UAV, and MEC at satellite respectively result in the energy consumption values of 0.1 MJ, 0.12 MJ, 97 MJ respectively. When K is taken as 30, the energy consumption values are observed to be 0.86 MJ, 0.94 MJ, 24.7 GJ respectively for the placement of MEC on ground, UAV and satellite. On average, the proposed solution achieves 9% improvement in the energy consumption when compared to placement of MEC at UAV and

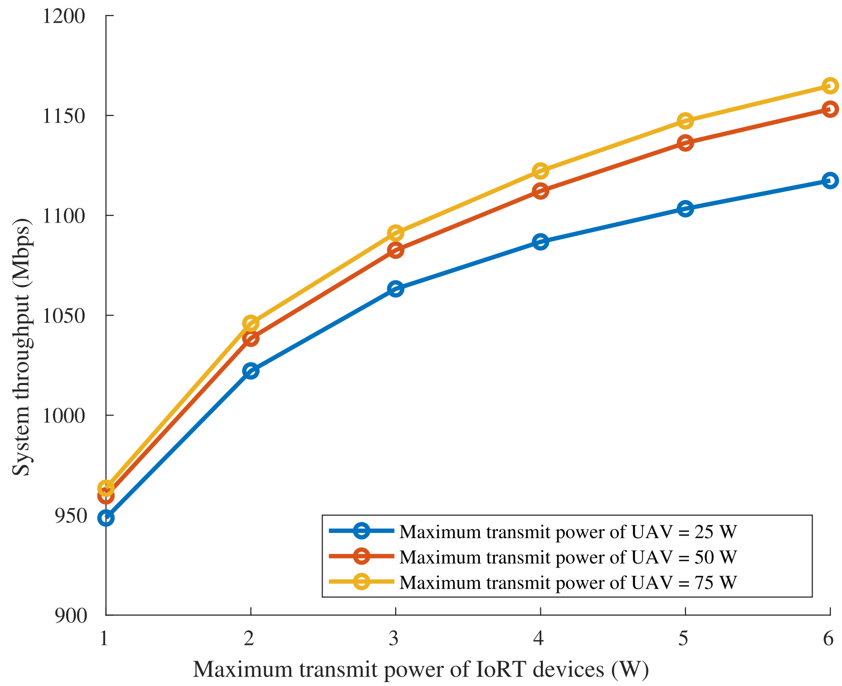

Fig. 10. System throughput (Mbps) vs maximum transmit power of IoRT devices (W).

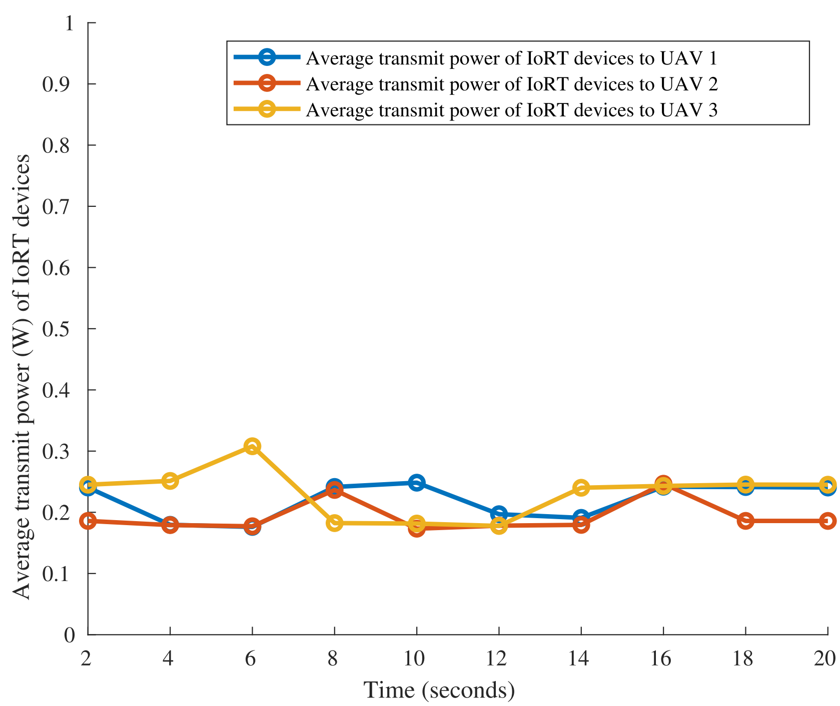

Fig. 11. Average transmit power (W) of IoRT devices.

99% improvement when compared to placement of MEC at the satellite. It can be seen that placing MEC at the satellite incurs largest energy consumption, followed by placing MEC on the UAV. The proposed solution i.e, placing MEC on the ground and using UAV as relays incurs lower energy consumption compared to the other two placements. As the distance between UAV and satellite is very large, the channel gain between the UAV and the satellite is very low. Hence, when MEC is placed at satellite, the UAV expends large amount energy to transmit the data. Alternately, placing the MEC and carrying out computations at the UAV results in increased energy consumption because of two reasons. First, the weight of UAV is increased because of carrying MEC device. It is results in increased energy consumption for flying of the UAV. Second, energy is expended for carrying the computations also. Further, the rapid depletion of energy at the UAV leads to increased frequency of trips to the charging station.

We also plotted the system throughput values for the three possible placement of MEC in Fig. 15. When the value of K is 5, the system throughput values observed for the placement of MEC on ground, at

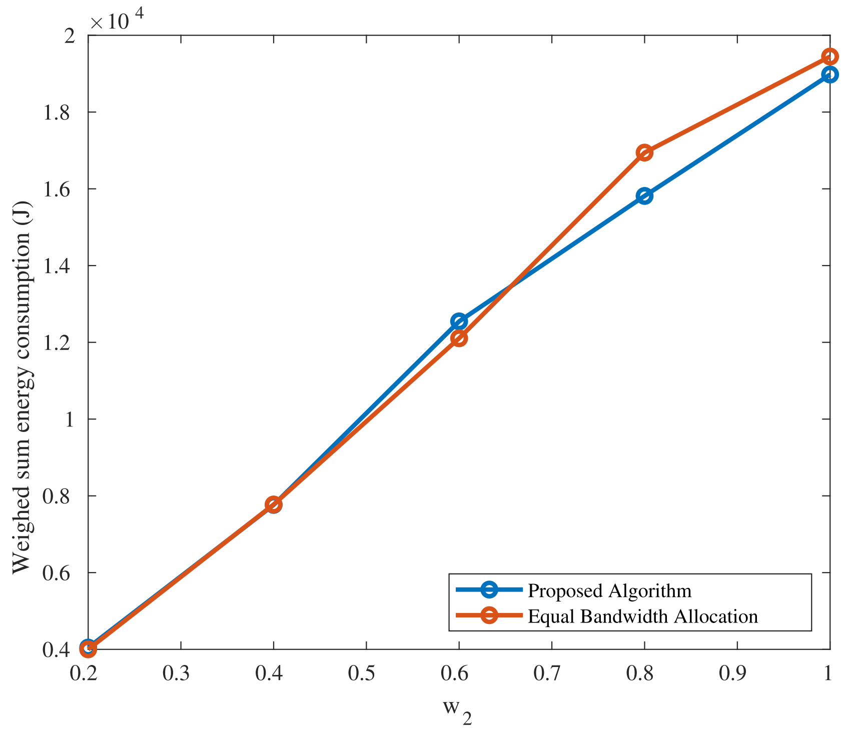

Fig. 12. Weighed sum energy consumption (J) of the UAVs and IoRT devices vs w_2.

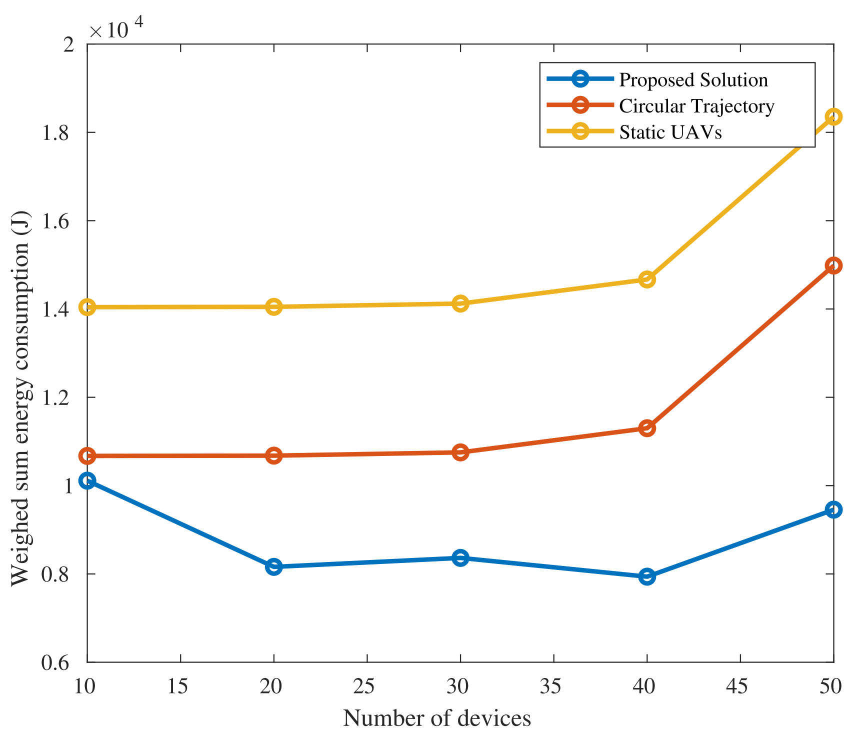

Fig. 13. Energy consumption vs number of devices for three different ways to design trajectories of the UAVs.

UAV and at the satellite respectively are 3028 Mbps, 3038 Mbps, and 1.6 Mbps respectively. When the number of devices is chosen as 30, the system throughput is observed to be 14085 Mbps, 14116 Mbps, and 9.5 Mbps respectively. As can be seen from Fig. 15, the proposed solution performs significantly better than the placement of UAV at the satellite. When compared to placement of MEC at the UAV, the proposed solution gives 0.2% lower system throughput on average. Placing MEC on satellite leads to lowest system throughput, which

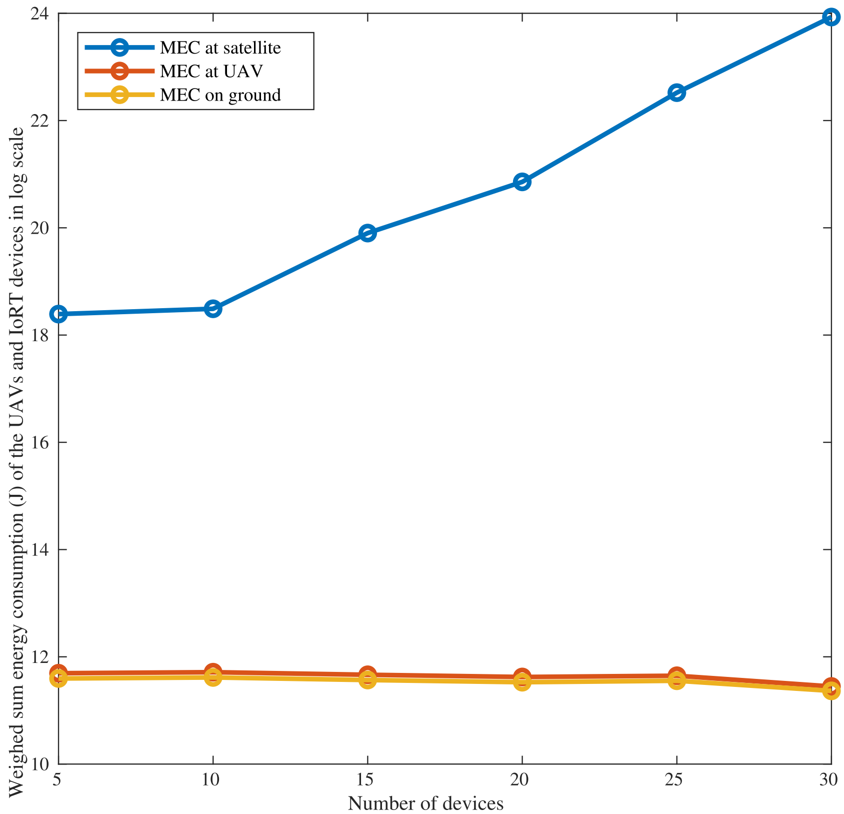

Fig. 14. Energy consumption vs number of devices for three different placements of MEC.

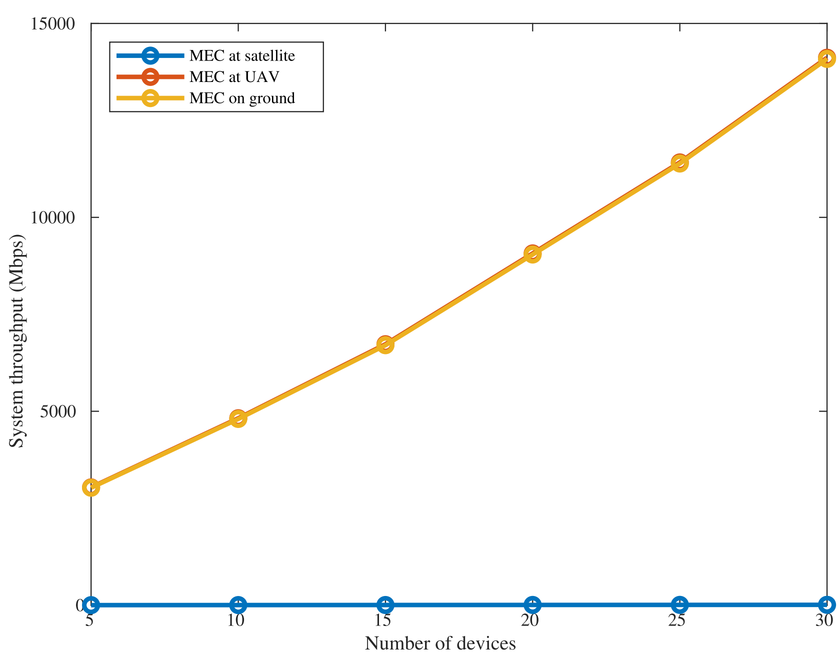

Fig. 15. System throughput vs number of devices for three different placements of MEC.

can be attributed to the fact the UAV should transmit the data over a very long distance when MEC is placed on the satellite. The proposed solution gives slightly lower system throughput compared to placing it at the UAV. This is because of the transmission that happens from UAV to the MEC device in the proposed solution, which is absent in placement of MEC at the UAV. However, the decrease in the system throughput is negligible compared to the significant gains in the energy consumption.

The presented results are based on the numerical simulations, for the use-case of providing MEC services to the energy-constrained IoRT devices. The solution is designed based on the assumptions of free-space path loss model, delay-tolerant data, and dominance of LoS links between UAVs and IoRT devices. Therefore, the proposed solution works best for the use case considered i.e., the IoRT devices spread over a remote area, lacking cellular infrastructure. For a non-remote scenario, appropriate path-loss models should be considered. Besides, the delay should be included in the objective when modeling the system for delay-sensitive data.

6. Conclusion

In this paper, we investigated the UAV-enabled MEC service provisioning architecture for remote IoRT devices, wherein the UAVs collect data from the IoRT devices and relay the collected data to the MEC device on the ground installed nearby. We optimized the dual objective of minimizing the energy consumption and maximizing the system throughput by jointly optimizing the connection scheduling, power control, bit transmission scheduling, bandwidth allocation, and UAVs' trajectories. Using numerical simulations, we showed that the proposed solution obtains significant performance improvement compared to the baseline schemes. In our future work, we plan to consider other Quality of Service parameters such as delay and reliability for the data collected from the IoRT devices. Another direction is to relax the requirement that the UAVs should always be in the line of sight of MEC device, so that larger geographical area can be served.

CRediT authorship contribution statement

Sriharsha Chigullapally: Conception and design of study, Acquisition of data, Analysis and/or interpretation of data, Writing – original draft. **C. Siva Ram Murthy:** Conception and design of study, Writing – review & editing.

Declaration of competing interest

The authors declare that they have no known competing financial interests or personal relationships that could have appeared to influence the work reported in this paper.

Data availability

No data was used for the research described in the article.

Acknowledgments

The authors would like to thank the PhD scholars at HPCN lab, IIT Madras - Vipin, Prabhu, Srinivasa and Vijay for several helpful discussions. This research work was supported by the Science and Engineering Research Board, New Delhi, India. Grant number: JBR/2021/000005. All authors approved the version of the manuscript to be published.

Appendix

The corresponding Lagrangian function can be expressed as:

$$\mathcal{L}^{(1)}(\mathbf{B},\rho) = \sum_{k=1}^{K}\sum_{m=1}^{M}\sum_{t=1}^{T}\Bigg\{\Bigg(w_1 c_{k,m}[t]E_{k,m}^{D\to U}[t] + w_2(E_{k,m}^{U\to M}[t] + c_{k,m}[t]E_{k,m}^{U\to K}[t])\Bigg) + \rho_{k,m,t}\Bigg(B_{k,m}^{D\to U}[t] + B_{k,m}^{U\to M}[t] + B_{k,m}^{U\to K}[t] - B\Bigg)\Bigg\}, \tag{41}$$

where $\rho = \{\rho_{k,m,t}, \forall k, m, t\}$ are the Lagrange multipliers associated with the corresponding constraints. Now, the Lagrangian dual function of the problem (31) can be presented as

$$\begin{aligned} d^{(1)}(\rho) = \min_{\mathbf{B}} \quad & \mathcal{L}^{(1)}(\mathbf{B},\rho) \\ s.t. \quad & (23q), (23u)\text{–}(23w) \end{aligned} \tag{42}$$

Hence, by applying Karush–Kuhn–Tucker (KKT) conditions, we can solve the problem (42).

References

[1] T. Huang, W. Yang, J. Wu, J. Ma, X. Zhang, D. Zhang, Survey on green 6G network: Architecture and technologies, IEEE Access 7 (2019) 175758–175768.

[2] Z. Li, Y. Wang, M. Liu, R. Sun, Y. Chen, J. Yuan, J. Li, Energy efficient resource allocation for UAV-assisted space-air-ground Internet of remote things networks, IEEE Access 7 (2019) 145348–145362.

[3] Y. Wang, Z. Li, Y. Chen, M. Liu, X. Lyu, X. Hou, J. Wang, Joint resource allocation and UAV trajectory optimization for space–air–ground Internet of remote things networks, IEEE Syst. J. 15 (4) (2021) 4745–4755.

[4] M. Liu, Y. Wang, Z. Li, X. Lyu, Y. Chen, Joint optimization of resource allocation and multi-UAV trajectory in space-air-ground IoRT networks, in: 2020 IEEE Wireless Communications and Networking Conference Workshops, WCNCW, 2020, pp. 1–6.

[5] L. Li, X. Wen, L. Zhaoming, Q. Pan, W. Jing, Z. Hu, Energy-efficient UAV-enabled MEC system: Bits allocation optimization and trajectory design, Sensors (Basel, Switzerland) 19 (2019).

[6] Y.K. Tun, Y.M. Park, N.H. Tran, W. Saad, S.R. Pandey, C.S. Hong, Energy-efficient resource management in UAV-assisted mobile edge computing, IEEE Commun. Lett. 25 (1) (2021) 249–253.

[7] X. Hu, K.-K. Wong, K. Yang, Z. Zheng, UAV-assisted relaying and edge computing: Scheduling and trajectory optimization, IEEE Trans. Wireless Commun. 18 (10) (2019) 4738–4752.

[8] Z. Yu, Y. Gong, S. Gong, Y. Guo, Joint task offloading and resource allocation in UAV-enabled mobile edge computing, IEEE Internet Things J. 7 (4) (2020) 3147–3159.

[9] Z. Jia, M. Sheng, J. Li, D. Niyato, Z. Han, LEO-satellite-assisted UAV: Joint trajectory and data collection for Internet of remote things in 6G aerial access networks, IEEE Internet Things J. 8 (12) (2021) 9814–9826.

[10] L. Abouzaid, E. Sabir, H. Elbiaze, A. Errami, O. Benhmammouch, The meshing of the sky: Delivering ubiquitous connectivity to ground Internet of Things, IEEE Internet Things J. 8 (5) (2021) 3743–3757.

[11] Z. Na, Y. Liu, J. Shi, C. Liu, Z. Gao, UAV-supported clustered NOMA for 6G-enabled Internet of Things: Trajectory planning and resource allocation, IEEE Internet Things J. 8 (20) (2021) 15041–15048.

[12] B. Chen, N. Li, Y. Li, X. Tao, G. Sun, Energy efficient hybrid offloading in space-air-ground integrated networks, in: 2022 IEEE Wireless Communications and Networking Conference, WCNC, 2022, pp. 1319–1324.

[13] T. Ren, J. Niu, B. Dai, X. Liu, Z. Hu, M. Xu, M. Guizani, Enabling efficient scheduling in large-scale UAV-assisted mobile-edge computing via hierarchical reinforcement learning, IEEE Internet Things J. 9 (10) (2022) 7095–7109.

[14] X. Zhou, L. Huang, T. Ye, W. Sun, Computation bits maximization in UAV-assisted MEC networks with fairness constraint, IEEE Internet Things J. (2022) 1.

[15] Q.-V. Pham, M. Le, T. Huynh-The, Z. Han, W.-J. Hwang, Energy-efficient federated learning over UAV-enabled wireless powered communications, IEEE Trans. Veh. Technol. 71 (5) (2022) 4977–4990.

[16] Z. Yang, S. Bi, Y.-J.A. Zhang, Online trajectory and resource optimization for stochastic UAV-enabled MEC system, IEEE Trans. Wireless Commun. (2022) 1.

[17] M. Zhao, W. Li, L. Bao, J. Luo, Z. He, D. Liu, Fairness-aware task scheduling and resource allocation in UAV-enabled mobile edge computing networks, IEEE Trans. Green Commun. Netw. 5 (4) (2021) 2174–2187.

[18] Y. Xu, T. Zhang, J. Loo, D. Yang, L. Xiao, Completion time minimization for UAV-assisted mobile-edge computing systems, IEEE Trans. Veh. Technol. 70 (11) (2021) 12253–12259.

[19] Z. Liao, Y. Ma, J. Huang, J. Wang, J. Wang, HOTSPOT: A UAV-assisted dynamic mobility-aware offloading for mobile-edge computing in 3-D space, IEEE Internet Things J. 8 (13) (2021) 10940–10952.

[20] C. Zhan, H. Hu, Z. Liu, Z. Wang, S. Mao, Multi-UAV-enabled mobile-edge computing for time-constrained IoT applications, IEEE Internet Things J. 8 (20) (2021) 15553–15567.

[21] E.E. Haber, H.A. Alameddine, C. Assi, S. Sharafeddine, UAV-aided ultra-reliable low-latency computation offloading in future IoT networks, IEEE Trans. Commun. 69 (10) (2021) 6838–6851.

[22] H. Ke, H. Wang, W. Sun, H. Sun, Adaptive computation offloading policy for multi-access edge computing in heterogeneous wireless networks, IEEE Trans. Netw. Serv. Manag. 19 (1) (2022) 289–305.

[23] Y. Xu, T. Zhang, Y. Liu, D. Yang, L. Xiao, M. Tao, UAV-assisted MEC networks with aerial and ground cooperation, IEEE Trans. Wireless Commun. 20 (12) (2021) 7712–7727.
[24] K. Zhang, X. Gui, D. Ren, D. Li, Energy–latency tradeoff for computation offloading in UAV-assisted multiaccess edge computing system, IEEE Internet Things J. 8 (8) (2021) 6709–6719.
[25] X. Gu, G. Zhang, M. Wang, W. Duan, M. Wen, P.-H. Ho, UAV-aided energy-efficient edge computing networks: Security offloading optimization, IEEE Internet Things J. 9 (6) (2022) 4245–4258.
[26] B. Dai, J. Niu, T. Ren, Z. Hu, M. Atiquzzaman, Towards energy-efficient scheduling of UAV and base station hybrid enabled mobile edge computing, IEEE Trans. Veh. Technol. 71 (1) (2022) 915–930.
[27] Z. Yu, Y. Gong, S. Gong, Y. Guo, Joint task offloading and resource allocation in UAV-enabled mobile edge computing, IEEE Internet Things J. 7 (4) (2020) 3147–3159.
[28] L. Zhang, N. Ansari, Latency-aware IoT service provisioning in UAV-aided mobile-edge computing networks, IEEE Internet Things J. 7 (10) (2020) 10573–10580.
[29] I. Azam, M.B. Shahab, S.Y. Shin, Energy-efficient pairing and power allocation for NOMA UAV network under QoS constraints, IEEE Internet Things J. (2022).
[30] J. Ji, K. Zhu, C. Yi, D. Niyato, Energy consumption minimization in UAV-assisted mobile-edge computing systems: Joint resource allocation and trajectory design, IEEE Internet Things J. 8 (10) (2021) 8570–8584.
[31] Y. Luo, W. Ding, B. Zhang, Optimization of task scheduling and dynamic service strategy for multi-UAV-enabled mobile-edge computing system, IEEE Trans. Cogn. Commun. Netw. 7 (3) (2021) 970–984.
[32] Q. Wu, Y. Zeng, R. Zhang, Joint trajectory and communication design for multi-UAV enabled wireless networks, IEEE Trans. Wireless Commun. 17 (3) (2018) 2109–2121.
[33] LTE unmanned aircraft systems trial report, Qualcomm Technol. (2017).
[34] D. Liu, Y. Xu, Y. Xu, Q. Wu, J. Jing, Y. Zhang, A. Anpalagan, Distributed relay selection for heterogeneous UAV communication networks using a many-to-many matching game without substitutability, in: 2017 IEEE/CIC International Conference on Communications in China, ICCC, 2017, pp. 1–6.
[35] T.M. Cover, J.A. Thomas, Elements of Information Theory (Wiley Series in Telecommunications and Signal Processing), Wiley-Interscience, USA, 2006.
[36] Q. Hu, Y. Cai, G. Yu, Z. Qin, M. Zhao, G.Y. Li, Joint offloading and trajectory design for UAV-enabled mobile edge computing systems, IEEE Internet Things J. 6 (2) (2019) 1879–1892.
[37] S. Boyd, L. Vandenberghe, Convex Optimization, Cambridge University Press, 2004.
[38] R.M. Corless, G.H. Gonnet, D.E.G. Hare, D.J. Jeffrey, D.E. Knuth, On the Lambertw function, Adv. Comput. Math. 5 (1996) 329–359.
[39] F. Zhou, Y. Wu, R.Q. Hu, Y. Qian, Computation rate maximization in UAV-enabled wireless-powered mobile-edge computing systems, IEEE J. Sel. Areas Commun. 36 (9) (2018) 1927–1941.
[40] Y. Nesterov, A. Nemirovskii, Interior-Point Polynomial Algorithms in Convex Programming, Society for Industrial and Applied Mathematics, 1994.
[41] M.T. Nguyen, L.B. Le, Multi-UAV trajectory control, resource allocation, and NOMA user pairing for uplink energy minimization, IEEE Internet Things J. (2022).

Chigullapally Sriharsha received the B.Tech. degree in Information Technology from SRM University, India in 2015, and the M.Tech. degree in Computer Science and Engineering from IIT Kanpur, Kanpur, India, in 2017. He is currently pursuing the Ph.D. degree with the High Performance Computing and Networking Laboratory, IIT Madras, Chennai, India. His research interests include Beyond 5G and 6G wireless networks.

C. Siva Ram Murthy (F'12) received the B.Tech. degree in Electronics and Communication Engineering from Regional Engineering College (now National Institute of Technology), Warangal, India, in 1982, the M.Tech. degree in Computer Engineering from IIT Kharagpur, Kharagpur, India, in 1984, and the Ph.D. degree in computer science from IISc, Bangalore, India, in 1988. Since 1988, he has been with the Department of Computer Science and Engineering, IIT Madras, Chennai, India, where he is currently the Richard Karp Institute Chair Professor, as well as a Visiting Professor at IIT Hyderabad. His research interests include wireless networks, lightwave networks, real-time systems, and parallel and distributed computing.